

Development of JURA

– A simulation code for electrochemical processes in molten salt –

(Research Document)

March, 2003

Japan Nuclear Cycle Development Institute

Tokai work

本資料の全部または一部を複写・複製・転載する場合は、下記にお問い合わせください。

〒319-1184 茨城県那珂郡東海村村松 4 番地 49
核燃料サイクル開発機構
技術展開部 技術協力課

電話:029-282-1122(代表)
ファックス:029-282-7980
電子メール:jserv@jnc.go.jp

Inquiries about copyright and reproduction should be addressed to:
Technical Cooperation Section,
Technology Management Division,
Japan Nuclear Cycle Development Institute
4-49 Muramatsu, Tokai-mura, Naka-gun, Ibaraki 319-1184,
Japan

© 核燃料サイクル開発機構 (Japan Nuclear Cycle Development Institute)
2003

Development of JURA

– A simulation code for electrochemical processes in molten salt –
(Research Document)

Tsuguyuki Kobayashi

Abstract

A simulation code for electrochemical processes in molten salt named JURA has been developed. This code can simulate the time history of the processes such as the metal pyro-process and the oxide pyro-process by the diffusion layer theory at various temperature and melts. This report describes the specific formulations of the theory for various electrodes such as the solid cathode, the Cd cathode, and the Cd pool anode. Explanation of the input data and sample calculations of the solid cathode, the Cd cathode as well as the MOX co deposition experiments are also given.

J U R A の開発

- 溶融塩中の電気化学過程のシミュレーションコード - (研究報告)

小林 嗣幸

要旨

溶融塩中の電気化学過程のシミュレーションコード J U R A を開発した。このコードは、金属電解法や酸化物電解法等のさまざまな温度や溶融塩中におけるプロセスの時間変化を拡散層理論によってシミュレートすることができる。この報告では固体陰極、カドミウム陰極、カドミウムプール陽極等のさまざまな電極の具体的な理論式を説明する。また、固体陰極、カドミウム陰極、M O X 共析の試験に対する入力データやサンプル計算に対する説明も加えた。

Table of contents

1. Introduction	1
2. Description of JURA code	2
2.1 Electrode models for the metallic fuel electro-refining	2
2.2 Electrode models for the oxide fuel electrolysis	7
3. Input data	17
4. Sample calculations	24
5. References	40

List of tables and figures

Table 3-1	Input data	21
Fig. 2-1	Electrorefining of spent metallic fuel	10
Fig. 2-2	Diffusion layer model of the solid cathode	11
Fig. 2-3	Calculation flow of the cathode potential & current Components in JURA code	12
Fig. 2-4	Diffusion layer model of the Cd cathode	13
Fig. 2-5	Diffusion layer model of the anodic dissolution	14
Fig. 2-6	Diffusion layer model of the Cd pool anode.....	15
Fig. 2-7	Electrolysis of spent oxide fuel	16
Fig. 4-1	Time history of Cell voltage in MOX co-deposition	25
Fig. 4-2	Time history of Anode current in MOX co-deposition	26
Fig. 4-3	Time history of Cathode current in MOX co-deposition	27
Fig. 4-4	Time history of salt concentration in MOX co-deposition	28
Fig. 4-5	Time history of cathode deposit in MOX co-deposition.....	29
Fig. 4-6	Time history of Pu enrichment in MOX co-deposition	30
Fig. 4-7	Time history of Cell voltage in Solid cathode deposition	31
Fig. 4-8	Time history of Anode current in Solid cathode deposition	32
Fig. 4-9	Time history of Cathode current in Solid cathode deposition	33
Fig. 4-10	Time history of salt concentration in solid cathode deposition...	34
Fig. 4-11	Time history of Cd pool concentration in solid cathode deposition.....	35
Fig. 4-12	Time history of cathode deposit in solid cathode deposition	36
Fig. 4-13	Time history of salt concentration in Cd cathode deposition	37
Fig. 4-14	Time history of Cd pool concentration in Cd cathode deposition.....	38
Fig. 4-15	Time history of cathode deposit in Cd cathode deposition	39

1. Introduction

Simulation codes are very important for the following reasons.

- a) They help us to decide the optimum experimental conditions by predicting the results under given experimental conditions.
- b) They help us to understand the experimental results by estimating immeasurable quantity such as components of each ion current in the observed total electric current.
- c) They help us to estimate the effects of process improvement.
- d) They help us to design the optimum electro-refiners for experimental facilities as well as those for commercial plants.
- e) They help us to evaluate the consistency of property data such as relative difference of standard potentials among the ions in the melt.

The author developed several simulation codes such as PALEO¹⁾, DEVON²⁾, and TRIAS etc. Advanced features of JURA* code are currently as follows.

- a) It can simulate both the metal pyro-process and the oxide pyro-process by the same diffusion layer model.
- b) It can calculate the electro-refining processes in different temperature conditions by reflecting the temperature dependence of the property data.
- c) Users can input their favorite property data in the input.
- d) It can calculate the processes in different melts.
- e) It can check the consistency of the property data recommended by ANL, RIAR and CRIEPI.
- f) Its calculation routines are written by “C” in Code Warrior’s IDE (Integrated Developmental Environments) and its plotting routines are written by “JAVA” in J Builder’s IDE so that JURA code can be modified and executed both in Mac OS X and Windows XP.

* JURA stands for JNC’s universal tool for actinides electro-refining.

2. Description of JURA code

JURA code can simulate the electrochemical processes of the metal pyro-process as well as the oxide pyro-process. The former process was originally developed by ANL* in USA to recycle the metallic fuel in the Integrated Fast Reactor concept while the latter one has been developed by RIAR** Russia for recycling the vibropac oxide fuel in a Fast Reactor. These processes differ in their temperature, the molten salt (melt), and the ion oxidation states but the same diffusion layer model based on the Nernst Eq. Will hold. JURA code is programmed to apply not only to these two processes but also to any other processes where the diffusion layer approximation remains appropriate.

2.1 Electrode models for the metallic fuel electro-refining³⁾

A typical electro-refining step in the metal pyro-process is shown in Fig. 2-1 where spent metallic fuels are dissolved by the anodic dissolution into the 3LiCl-2KCl melt at 773 K and only U deposits on the solid cathode and then both U and Pu deposit into the liquid Cd cathode.

(1) Solid cathode model

Solid cathode is made of low carbon steel immersed in the 3LiCl-2KCl salt to deposit only U in the melt. The deposited U is dendritic and contains a lot of salt. At 773 K, the reduction process is expected to be very fast so that the surface concentration of the ion is in equilibrium. Hence the following Nernst Eq. (2-1) holds.

$$E_{sc} = E_f^x + \frac{R \cdot T}{Z_x \cdot F} \ln \left(\frac{X_{sc}^{salt}}{a_x^{sc}} \right) \quad (2-1)$$

Where

E_{sc} : Potential of solid cathode (V vs. Cl/Cl₂)

E_f^x : Formal standard potential of ion X (V vs. Cl/Cl₂); $E_f^x = E_0^x + \frac{R \cdot T}{Z_x \cdot F} \ln(g_{sc}^{salt})$

E_0^x : Standard potential of ion X (V vs. Cl/Cl₂)

R : Gas constant (= 8.314 J/mol/K)

T : Temperature (K)

Z_x : Number of equivalents per mole of ion x

F : Faraday constant (= 96485 C/mol)

X_{sc}^{salt} : Surface concentration of ion X on the cathode (mol fraction)

a_x^{sc} : Activity of element X in the solid cathode deposit

* Argonne National Laboratory

** Research Institute of Atomic Reactor

By using Eq. (2-1), the concentration on the cathode surface can be calculated by the following Eq. (2-2).

$$X_{sc}^{salt} = a_x^{sc} \exp \left\{ -\frac{Z_x \cdot F}{R \cdot T} (E_f^x - E_{sc}) \right\} \quad (2-2)$$

In the diffusion layer model, concentration of ions on the cathode surface changes within the diffusion layer as shown in Fig. 2-2. Then the current component of ion x can be calculated by the diffusion mass transfer by the concentration gradient as the following Eq.

$$e_{sc} \cdot j_x = S_{sc} \cdot F \cdot Z_x \cdot D_x^{salt} \cdot \frac{(X_b^{salt} - X_{sc}^{salt})}{d_{sc}^{salt}} \cdot \frac{\mathbf{r}^{salt}}{M^{salt}} \quad (2-3)$$

Where

- e_{sc} : Solid cathode current efficiency
- S_{sc} : Effective area of the solid cathode (cm²)
- D_x^{salt} : Diffusion coefficient of ion x in the salt (cm²/s)
- X_b^{salt} : Bulk concentration of ion X in the salt (mol fraction)
- d_{sc}^{salt} : Diffusion layer thickness (cm)
- \mathbf{r}^{salt} : Density of the salt (g/cm³)
- M^{salt} : Molecular weight of the salt (g/mol)

The cathode potential is determined by iteration until the summation of the current components of the ions meets with the given total current as follows. The program flow is shown in Fig. 2-3.

$$I_{tot} = \sum_x j_x \quad (2-4)$$

Electrochemical Reduction of U³⁺, Pu³⁺, Np³⁺, Am³⁺, Cm³⁺, Ce³⁺, Nd³⁺, La³⁺, Gd³⁺, Zr³⁺, Cd³⁺, and Li⁺ ions at the solid cathode are considered.

(2) Cd cathode model

Cd cathode consists of a ceramic crucible filled with the liquid Cd immersed in the 3LiCl-2KCl melt to deposit both U and Pu ions in the melt. The deposited U and Pu dissolved into the liquid Cd. By assuming the equilibrium, the following Nernst Eq. holds.

$$E_{cc} = E_f^x + \frac{R \cdot T}{Z_x \cdot F} \ln \left(\frac{X_{cc}^{salt}}{\mathbf{g}_x^{Cd} \cdot X_{cc}^{Cd}} \right) \quad (2-5)$$

Where

E_{cc} : Potential of Cd Cathode (V vs. Cl/Cl₂)

X_{cc}^{salt} : Surface concentration of ion X on the salt side of Cd cathode (mol fraction)

γ_x^{Cd} : Activity coefficient of element X in the Cd

X_{cc}^{Cd} : Concentration of element X on the Cd side of Cd cathode surface (mol fraction)

In the diffusion layer model, the concentration of the ions changes into the bulk concentration within the diffusion layer as shown in Fig. 24. When the mass transfer across the Cd cathode surface is continuous, the following Eq. holds.

$$D_x^{salt} \frac{(X_b^{salt} - X_{cc}^{salt})}{d_{cc}^{salt}} \cdot \frac{r^{salt}}{M^{salt}} = D_x^{Cd} \frac{(X_{cc}^{Cd} - X_b^{Cd})}{d_{cc}^{Cd}} \cdot \frac{r^{Cd}}{M^{Cd}} \quad (2-6)$$

Where

X_{cc}^{salt} : Surface concentration of ion X on the Cd cathode (mol fraction)

D_x^{salt} : Diffusion coefficient of ion X in the salt side of the Cd cathode (mol fraction)

d_{cc}^{salt} : Diffusion layer thickness in the salt side of the Cd cathode (cm)

X_{cc}^{Cd} : Surface concentration of element x in the Cd side of the Cd cathode (mol fraction)

X_b^{Cd} : Bulk Concentration of element x in the Cd cathode (mol fraction)

d_{cc}^{Cd} : Diffusion layer thickness in the Cd side of the Cd cathode (cm)

r^{Cd} : Density of the Cd (g/cm³)

M^{Cd} : Molecular weight of the Cd (g/mol)

From Eq. (2-5), the following Eq. holds.

$$\frac{X_{cc}^{salt}}{X_{cc}^{Cd}} = g_x^{Cd} \cdot \exp\left\{\frac{Z_x \cdot F}{R \cdot T} (E_{cc} - E_f^x)\right\} = b_2 \quad (2-7)$$

From Eq. (2-6) the following Eq. holds.

$$X_{cc}^{Cd} - X_b^{Cd} = \frac{D_x^{salt} \cdot d_{cc}^{Cd} \cdot r^{salt} \cdot M^{Cd}}{D_x^{Cd} \cdot d_{cc}^{salt} \cdot r^{Cd} \cdot M^{salt}} (X_b^{salt} - X_{cc}^{salt}) = b_1 \cdot (X_b^{salt} - X_{cc}^{salt}) \quad (2-8)$$

By substituting Eq. (2-7) into Eq. (2-8) and rearranging, the surface concentration in the Cd side of the Cd cathode can be expressed as follows.

$$X_{cc}^{Cd} = \frac{X_b^{Cd} + b_1 \cdot X_b^{salt}}{1 + b_1 \cdot b_2} \quad (2-9)$$

If the calculated concentration is larger than the solubility limit of the element in Cd, the latter is used as the concentration. Then, the surface concentration in the salt side of the Cd cathode can be

calculated by Eq. (2-7). The Cd cathode potential is determined by the same manner with the solid cathode. Electrochemical reductions of U^{3+} , Pu^{3+} , Np^{3+} , Am^{3+} , Cm^{3+} , Ce^{3+} , Nd^{3+} , La^{3+} , Gd^{3+} , Zr^{3+} , Cd^{3+} , and Li^+ ions at the Cd cathode are considered.

(3) The anode basket model

An anode basket is made of low carbon steel immersed in the melt to anodically dissolve the spent metallic fuel into the salt. By assuming the equilibrium, the following Nernst Eq. holds.

$$E_{ab} = E_f^x + \frac{R \cdot T}{Z_x \cdot F} \ln \left(\frac{X_{ab}^{salt}}{a_x^{ab}} \right) \quad (2-10)$$

Where

E_{ab} : Potential of anode basket (V vs. Cl/Cl₂)

X_{ab}^{salt} : Surface concentration of ion X on the anode (mol fraction)

a_x^{sc} : Activity of element X in the spent fuel

By using Eq. (2-10), the concentration on the anode surface can be calculated by the following Eq.

$$X_{ab}^{salt} = a_x^{ab} \exp \left\{ - \frac{Z_x \cdot F}{R \cdot T} (E_f^x - E_{ab}) \right\} \quad (2-11)$$

In the diffusion layer model, the concentration of ions changes into the bulk concentration within the diffusion layer as shown in Fig. 2-5. Then, the current component of ion x can be calculated by the diffusion mass transfer by the concentration gradient as the following Eq.

$$e_{ab} \cdot j_x = S_{ab} \cdot F \cdot Z_x \cdot D_x^{salt} \cdot \frac{(X_{sab}^{salt} - X_b^{salt})}{d_{ab}^{salt}} \cdot \frac{r^{salt}}{M^{salt}} \quad (2-12)$$

Where

e_{ab} : Anode basket current efficiency

S_{ab} : Effective area of the anode basket (cm²)

d_{ab}^{salt} : Diffusion layer thickness on the surface of the anode basket (cm)

Then, the potential of the anode basket can be determined in the same manner with the solid cathode. Electrochemical oxidation of U^{3+} , Pu^{3+} , Np^{3+} , Am^{3+} , Cm^{3+} , Ce^{3+} , Nd^{3+} , La^{3+} , Gd^{3+} , Zr^{3+} , and Fe^{2+} ions from the anode basket are considered.

(4) The Cd pool anode model

A Cd pool anode consists of liquid Cd at the bottom of the electro-refiner, which chemically

dissolves the spent metallic fuel. The dissolved U and Pu will be anodically oxidized into the melt. By assuming the equilibrium, the following Nernst Eq. holds.

$$E_{ap} = E_f^x + \frac{R \cdot T}{Z_x \cdot F} \ln \left(\frac{X_{ap}^{salt}}{\mathbf{g}_x^{Cd} \cdot X_{ap}^{Cd}} \right) \quad (2-13)$$

Where

E_{ap} : Potential of Cd pool anode (V vs. Cl/Cl₂)

X_{ap}^{salt} : Surface concentration of ion X on the salt side of Cd pool (mol fraction)

X_{ap}^{Cd} : Concentration of element X on the Cd side of Cd pool surface (mol fraction)

In the diffusion layer model, the concentration of the ions changes into the bulk concentration within the diffusion layer as shown in Fig. 2-6. When the mass transfer across the Cd pool surface is continuous the following Eq. holds.

$$D_x^{salt} \frac{(X_b^{salt} - X_{ap}^{salt})}{\mathbf{d}_{ap}^{salt}} \cdot \frac{\mathbf{r}^{salt}}{M^{salt}} = D_x^{Cd} \frac{(X_{ap}^{Cd} - X_b^{ap})}{\mathbf{d}_{ap}^{Cd}} \cdot \frac{\mathbf{r}^{Cd}}{M^{Cd}} \quad (2-14)$$

Where

X_{ap}^{salt} : Surface concentration of ion X on the Cd pool (mol fraction)

D_x^{salt} : Diffusion coefficient of ion X in the salt side of the Cd pool (mol fraction)

\mathbf{d}_{ap}^{salt} : Diffusion layer thickness in the salt side of the Cd pool (cm)

X_{ap}^{Cd} : Surface concentration of element X in the Cd side of the Cd pool (mol fraction)

X_b^{ap} : Bulk Concentration of element X in the Cd pool (mol fraction)

\mathbf{d}_{ap}^{Cd} : Diffusion layer thickness in the Cd side of the Cd pool (cm)

From Eq. (2-13), the following Eq. holds.

$$\frac{X_{ap}^{salt}}{X_{ap}^{Cd}} = \mathbf{g}_x^{Cd} \cdot \exp \left\{ \frac{Z_x \cdot F}{R \cdot T} (E_{ap} - E_f^x) \right\} = \mathbf{a}_2 \quad (2-15)$$

From Eq. (2-14), the following Eq. holds.

$$X_{ap}^{Cd} - X_b^{ap} = \frac{D_x^{salt} \cdot \mathbf{d}_{ap}^{Cd} \cdot \mathbf{r}^{salt} \cdot M^{Cd}}{D_x^{Cd} \cdot \mathbf{d}_{ap}^{salt} \cdot \mathbf{r}^{Cd} \cdot M^{salt}} (X_b^{salt} - X_{ap}^{salt}) = \mathbf{a}_1 \cdot (X_b^{salt} - X_{ap}^{salt}) \quad (2-16)$$

By substituting Eq. (2-15) into Eq. (2-16) and rearranging, the surface concentration in the Cd side of the Cd pool can be expressed as follows.

$$X_{ap}^{Cd} = \frac{X_b^{ap} + a_1 \cdot X_b^{salt}}{1 + a_1 \cdot a_2} \quad (2-17)$$

If the calculated concentration is larger than the solubility limit of the element in Cd, the latter is used as the concentration. Then, the surface concentration in the salt side of the Cd cathode can be calculated by Eq. (2-15). The Cd pool potential is determined in the same manner with the solid cathode. Electrochemical oxidation of U^{3+} , Pu^{3+} , Np^{3+} , Am^{3+} , Cm^{3+} , Ce^{3+} , Nd^{3+} , La^{3+} , Gd^{3+} , Zr^{3+} , and Cd^{2+} ions from the anode pool are considered.

2.2 Electrode models for the oxide fuel electrolysis

The typical electrolysis step in the oxide pyro-process is shown in Fig. 2-7 where spent oxide fuels are dissolved by the anodic dissolution in the 2CsCl-NaCl salt at 923 K and only UO_2 are deposited on the graphite cathode. After oxidation of PuO_2 ions by oxygen gas purge both UO_2 and PuO_2 are deposit on the graphite cathode. These deposited granules have nearly the theoretical density and they can be used as the vibropac fuel after removing the adhered salt.

(1) The graphite cathode model

A graphite cathode model is the same as that of the solid cathode model. Electrochemical reductions of UO_2^{2+} , PuO_2^{2+} , NpO_2^{2+} , Am^{3+} , Cm^{3+} , Ce^{3+} , Nd^{3+} , La^{3+} , Gd^{3+} , Rh^{3+} , Pd^{3+} , Ru^{3+} , Fe^{2+} , and Li^+ at the graphite cathode are considered.

(2) The graphite anode model

A graphite anode model is the same as that of the anode basket model. Electrochemical oxidation of Cl at the graphite anode is considered.

(3) The anodic dissolution model

An anodic dissolution model is the same as that of the anode basket model but oxidation of UO_2^{2+} , NpO_2^{2+} , Rh^{3+} , Pd^{3+} , Ru^{3+} , Fe^{2+} , and Cl at the graphite anode is considered.

(4) The chlorination model

The following Eq calculates chlorination rate of the charged oxides.

$$\frac{dX^{salt}}{dt} = e_{cl} \cdot \frac{2}{Z_x} \cdot \frac{dV_{cl}}{dt} \quad (2-18)$$

Where

X^{salt} : Concentration of ion X in the salt (mol fraction)

t : time (s)

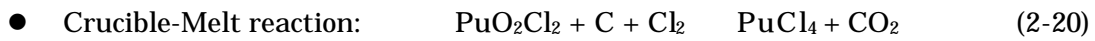
e_{cl} : Efficiency of the chlorination

V_{cl} : Volume of chlorine gas purge (litter)

Chlorination of UO_2^{2+} , PuO_2^{2+} , NpO_2^{2+} , Am^{3+} , Cm^{3+} , Ce^{3+} , Nd^{3+} , La^{3+} , Gd^{3+} , Rh^{3+} , Ru^{3+} , Pd^{2+} and Fe^{2+} ions by the chlorine gas purge is considered.

(5) Oxidation and reduction of Pu ion

The following reactions must be considered to predict the concentration of PuO_2^{2+} in the melt.



Based on the experimental observations⁴⁾ with UO_2^{2+} ions, the following equation is assumed to describe the concentration of PuO_2^{2+}

$$V \cdot \frac{dC_{Pu(6+)}}{dt} = S_G \cdot \frac{k_0 \cdot P_{O_2}}{k_{Cl_2} \cdot P_{Cl_2}^{1/2} + 1} - S_G \cdot k_{red} \cdot P_{Cl_2} \cdot C_{Pu(6+)} - S_C \cdot k_c \cdot P_{Cl_2} \cdot C_{Pu(6+)} - \frac{i_{Pu(6+)} \cdot 60}{z \cdot F} \quad (2-22)$$

where

V: volume of the melt (cm³)

$C_{Pu(6+)}$: concentration of PuO_2^{2+} (mol/cm³)

t: Time (min)

S_G : interreaction area between the process gas and melt(cm²)

k_0 : Rate constant (mol/min/cm²/Pa)

P_{O_2} : Oxygen pressure (Pa)

k_{Cl_2} : Rate constant (Pa^{-1/2})

P_{Cl_2} : Chlorine pressure (Pa)

k_{red} : Rate constant of the reverse reaction (2-19) (cm/min/Pa)

S_C : Interaction area between the crucible and the melt (cm²)

k_c : Rate constant of the reaction (2-20) (cm/min/Pa)

$i_{Pu(6+)}$: Cathode current component of the reaction (2-21) (A)

z: mole equivalent of $PuO_2^{2+} = 2$

F: Faraday constant = 96500 C/mol

The rate constants for the reaction (2-22) were evaluated as follows by a very small laboratory experiment ^{4),7)}.

$$\log_{10}(k_0) = -6.15 - 3.5 \times 10^3/T(\text{K})$$

$$\log_{10}(k_{\text{Cl}_2}) = -0.80 - 1.5 \times 10^3/T(\text{K})$$

$$\log_{10}(k_{\text{red}}) = -1.844 - 4780/T(\text{K})$$

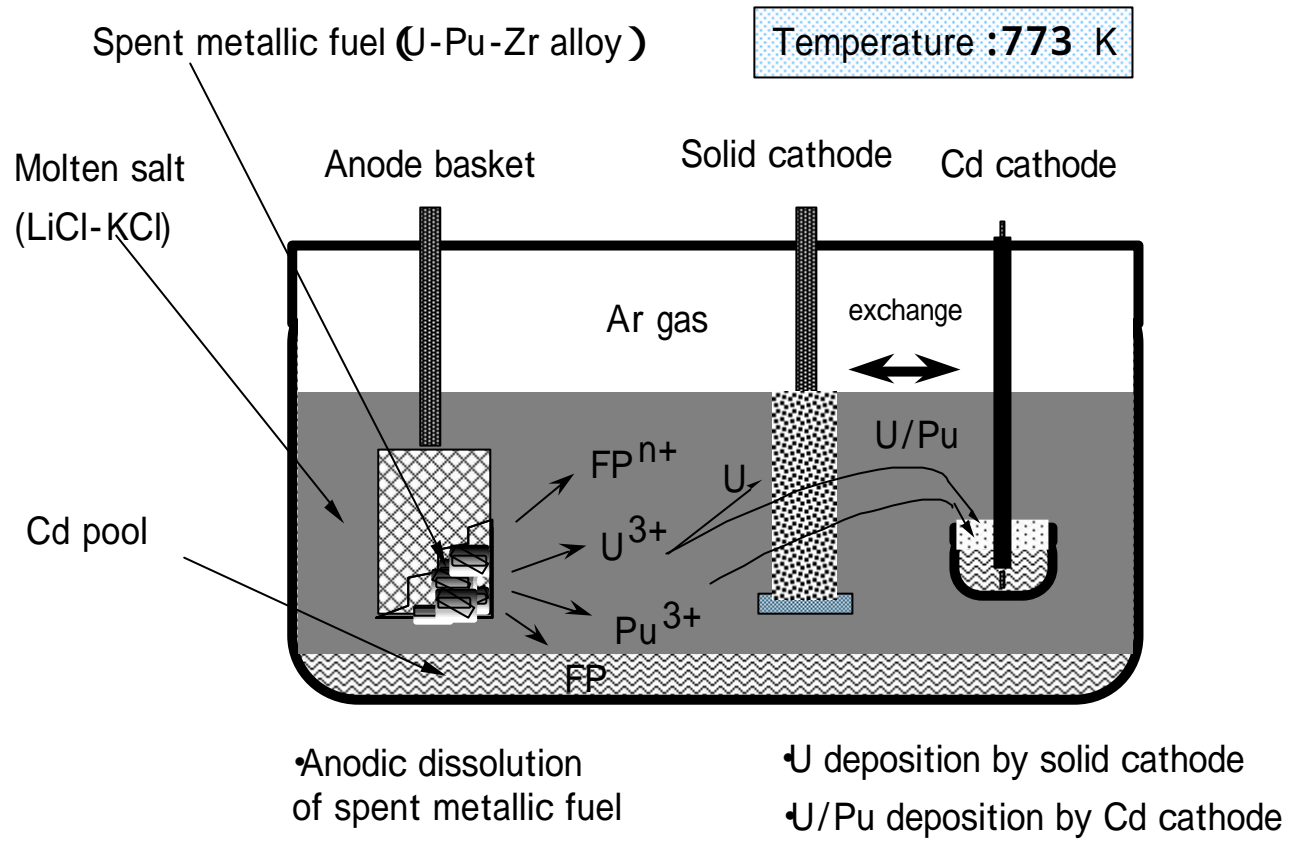


Fig. 2-1 Electro-refining of spent metallic fuel

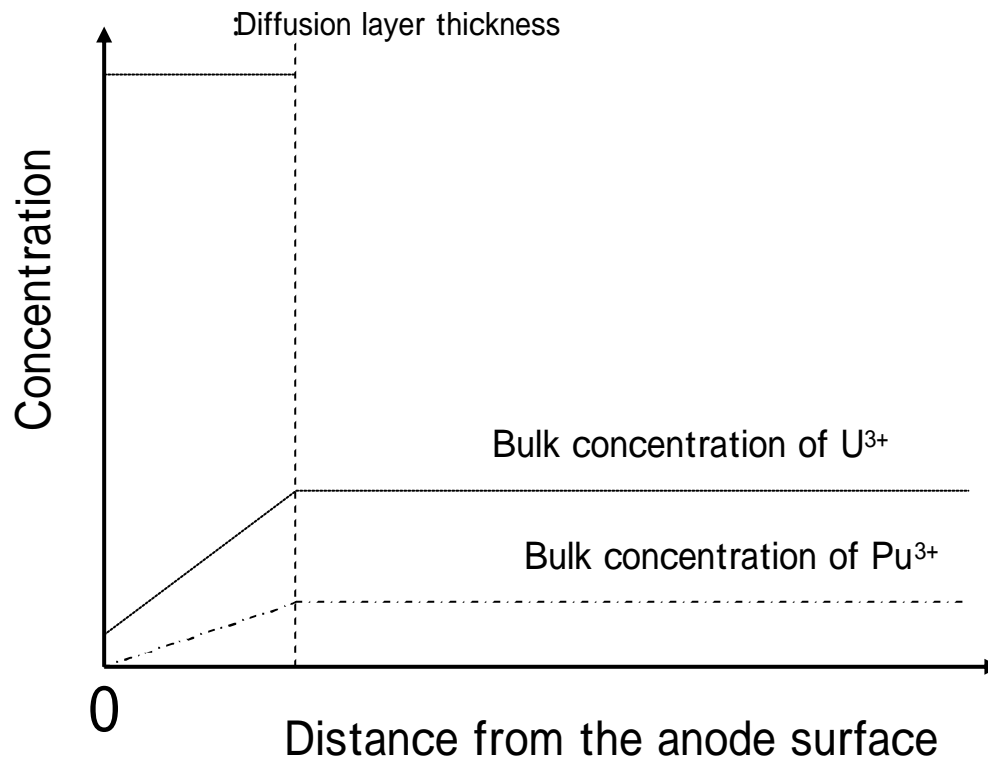


Fig. 2-2 Diffusion layer model of the solid cathode

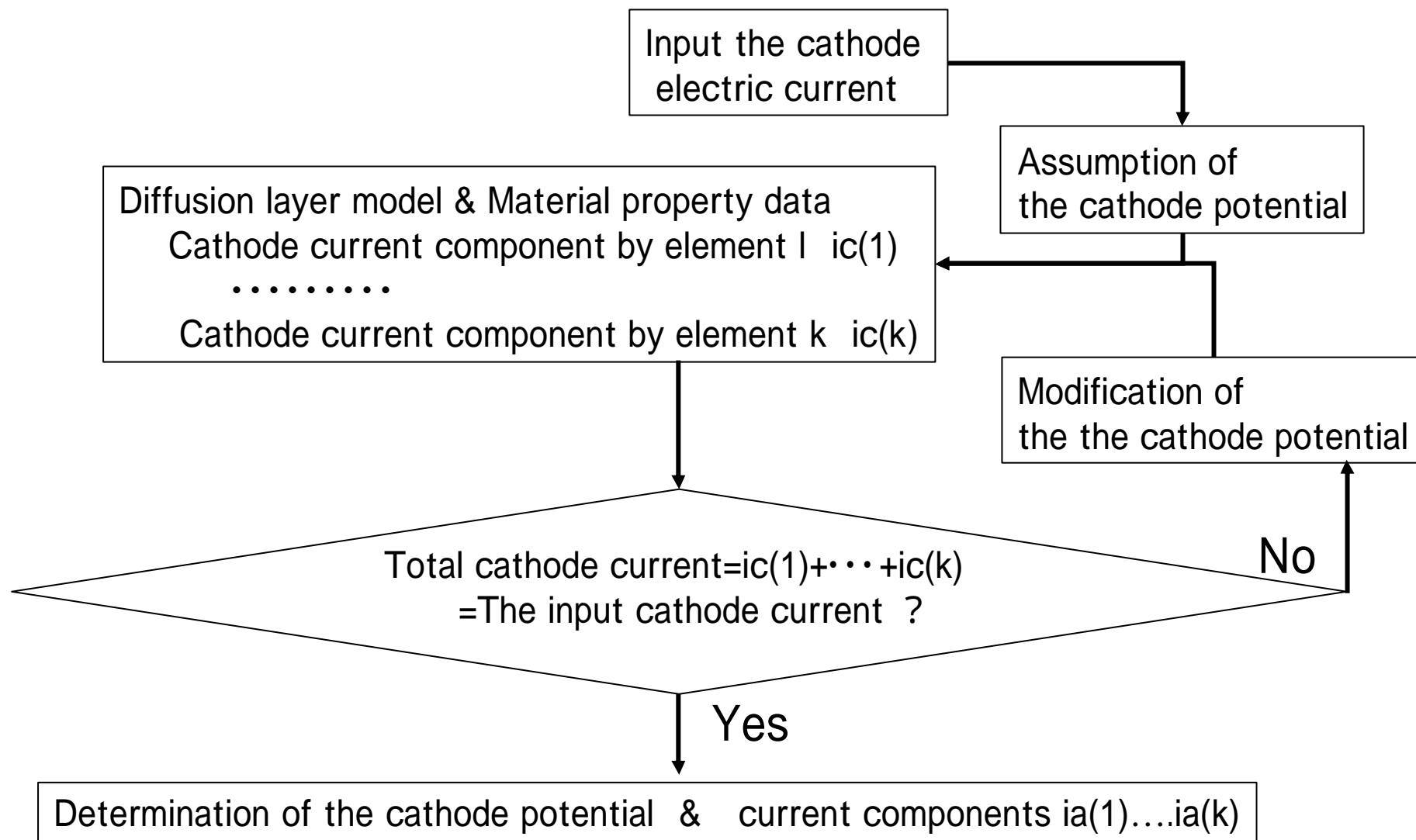


Fig. 2-3 Calculation flow of the cathode potential & current compenents in JURA code

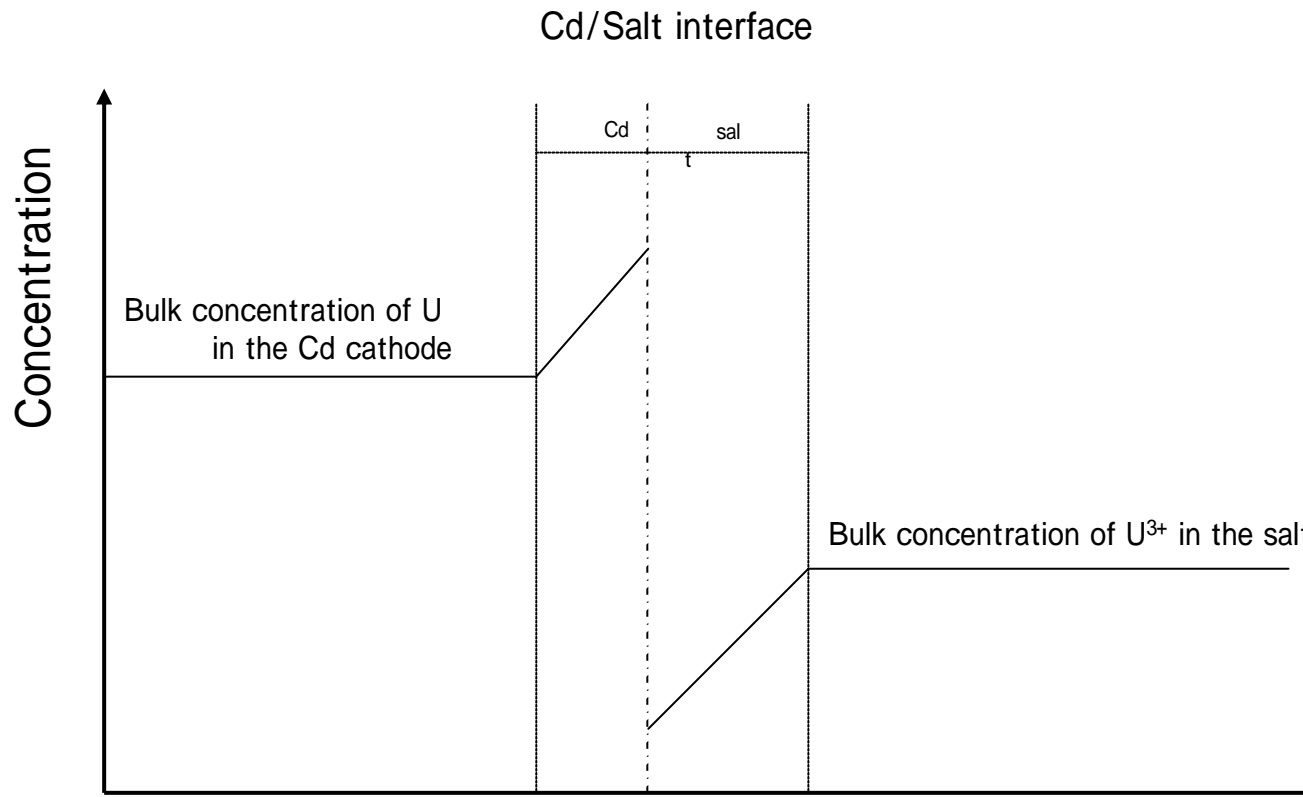


Fig. 2-4 Diffusion layer model of the Cd cathode

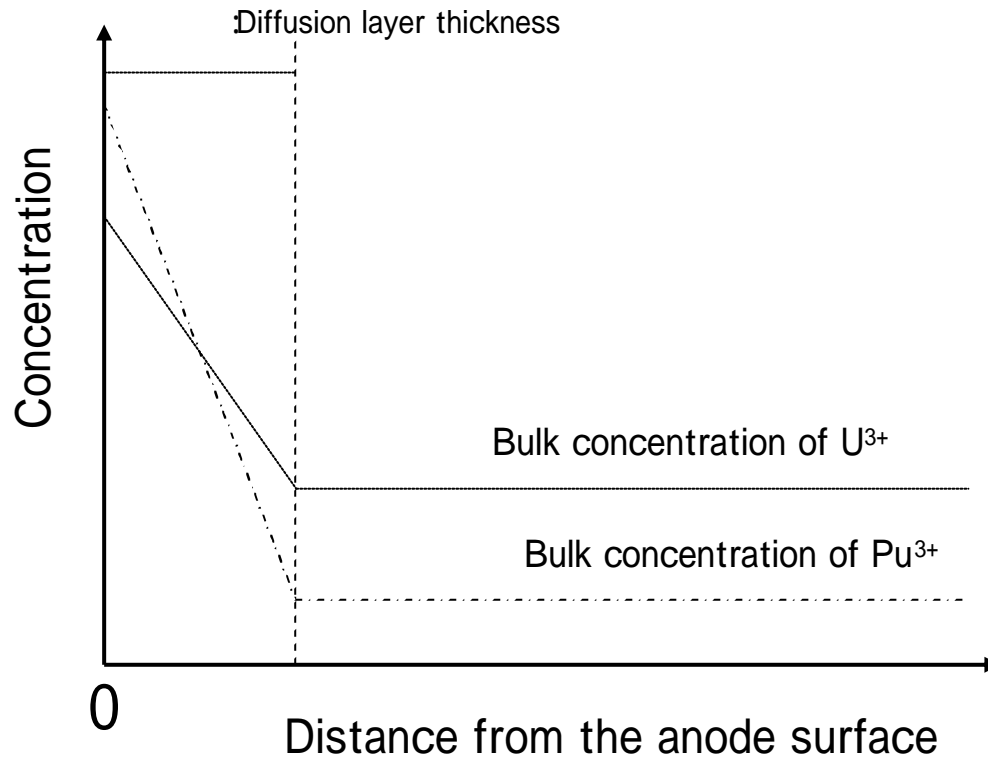


Fig.2-5 Diffusion layer model of the anodic dissolution

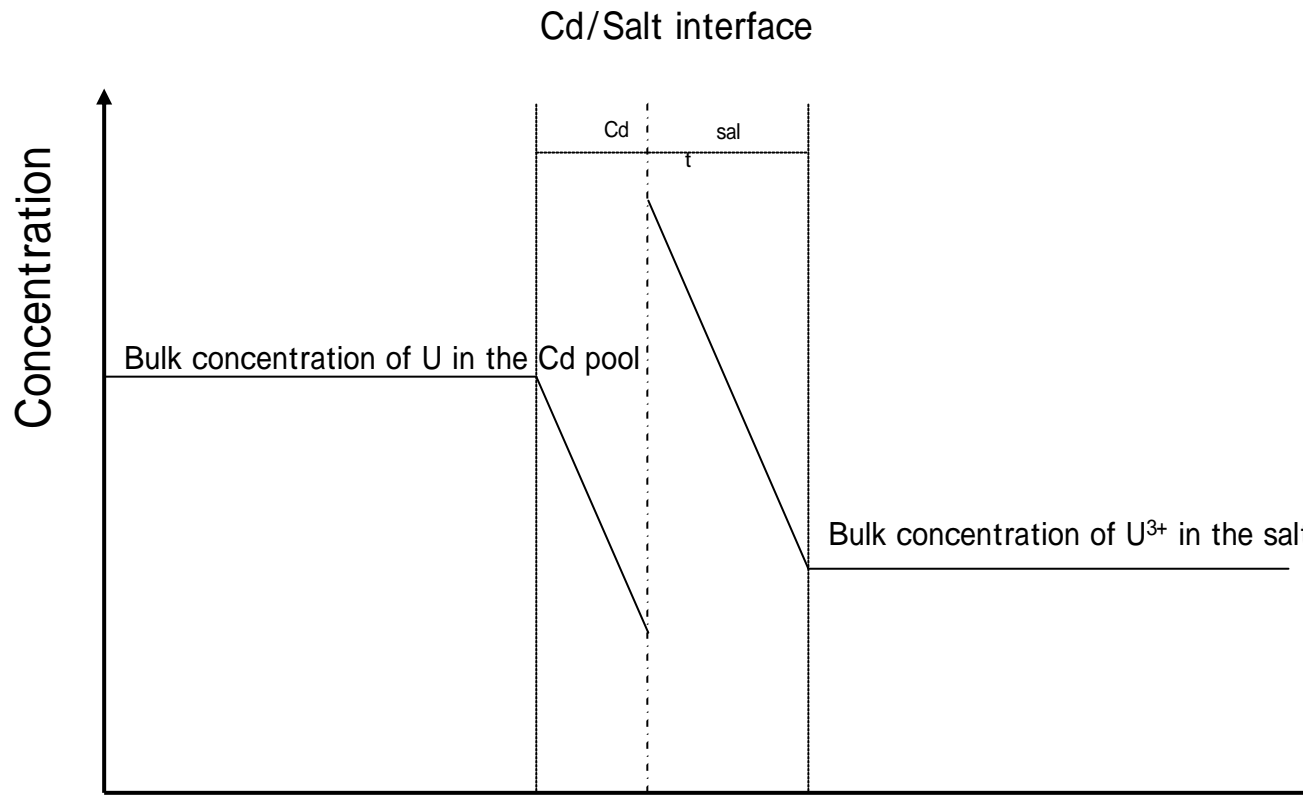


Fig. 2-6 Diffusion layer model of the Cd pool anode

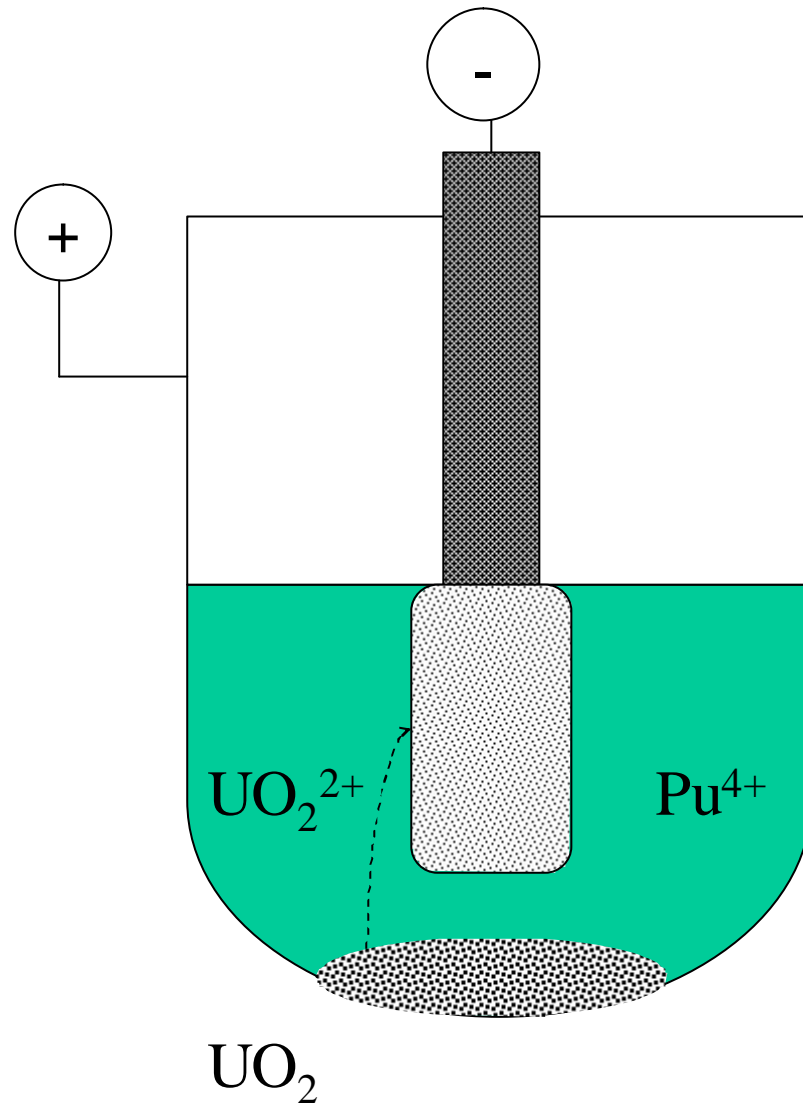


Fig.2-7 Electrolysis spent oxide fuel

3. Input data

The input data of JURA code are shown in Table 3-1. The followings are explanation of each line.

- (1) Line #1: Title of the calculation that appears in the plotting.
- (2) Line #2: Temperature of salt given in the unit of Kelvin.
- (3) Line #3 - 13:

Appropriate formal potential of UO_2 , U, PuO_2 , Pu, NpO_2 , Np, Am, Cm, RE1, RE2, and NM ions will be used in JURA where RE1 and RE2 can be selected from Ce, Nd, La, Gd and NM from Rh, Ru and Pd ions. The number of mole equivalents of the ion can be given by z . For example, $z = +2$ for UO_2^{2+} and $z = +3$ for Pu^{3+} . The temperature dependence of formal potential E_f can be given by **a** and **b** in the following formula where the reference is the potential of Cl/Cl_2 electrode.

$$E_f (\text{V}) = \mathbf{a} + \mathbf{b} \cdot T(\text{K})/1000 \quad (3-1)$$

A specific formal potential E_f^* at certain temperature can be input by $\mathbf{a} = E_f^*$ and $\mathbf{b} = 0$.

The diffusion constant D of the ion is given by **A** and **B** in the following formula.

$$D(\text{cm}^2/\text{s}) = \mathbf{A} \exp(-\mathbf{B} / T(\text{K})) \quad (3-2)$$

A specific diffusion constant D^* can be given by $\mathbf{A} = D^*$ and $\mathbf{B} = 0$.

- (4) Line #14: Surface area of the following anode in the unit of cm^2 .

Sa: Cd pool, **Sb**: Anode basket, **ScdLi**: Cd-Li anode, **Sw**: Zr deposit on ER wall as anode

- (5) Line #15: Surface area of the following cathode in the unit of cm^2 .

Sc: Solid cathode, **Scd**: Cd cathode

- (6) Line #16: Multiply factor to the surface area in the Cd pool dissolution calculation

- (7) Line #17: Diffusion layer thickness of the following anode in the unit of cm.

dLBkt: Anode basket, **dLCdcl**: Cd pool salt side, **dLCdcd**: Cd pool Cd side, **dLWcl**: ER wall for Zr anode

- (8) Line #18: Diffusion layer thickness of the following cathode in the unit of cm.

dLSld: Solid cathode, **dLCdcl**: Cd cathode salt side, **dLCdcd**: Cd cathode Cd side

- (9) Line #19: Selection of one of the lanthanide 1=Ce; 2=Nd; 3=La; 4=Gd

- (10) Line #20: Selection of the other lanthanide 1=Ce; 2=Nd; 3=La; 4=Gd

- (11) Line #21: Selection of noble metal 1=Rh; 2=Ru; 3=Pd

- (12) Line #22 - 31: Initial weight of the following charge into the ER

#22 **UOsfi**: UO_2 , **Usfi**: U

#23 **PuOsfi**: PuO_2 , **Pusfi**: Pu

#24 **NpOsfi**: NpO_2 , **Npsfi**: Np

#25 **Amsfi:** Am

#26 **Cmsfi:** Cm

#27 **RE1sfi:** RE1

#28 **RE2sfi:** RE2

#29 **NMsfi:** Noble metal

#30 **Zrsfi:** Zr

#31 **Fesfi:** Fe

(13) Line #32: Total Salt inventory in the ER in the unit of gram

(14) Line #33: Total Cd inventory in Cd pool in the unit of gram

(15) Line #34: Amount of Cd charge in the Cd cathode in the unit of gram

(16) Line #35: Amount of Cd-Li charge in Cd-Li anode in the unit of gram

(18) Line #36: Selection of the following salt

1=LiCl-KCl; 2=NaCl-KCl; 3=NaCl-2CsCl; 4=NaCl-KCl-CsCl

(19) Line #37 - 48: Initial concentration of the followings in the unit of weight %

#37 **xUOcli:** UO₂ in salt, **xUcli:** U in salt, **xUcdpi:** U in Cd pool

#38 **xPuOcli:** PuO₂ in salt, **xPucli:** Pu in salt, **xPucdpi:** Pu in Cd pool

#39 **xNpOcli:** NpO₂ ion, **xNpcli:** Np ion, **xNcdpi:** Np in Cd pool

#40 **xAmcli:** Am in salt, **xAmedpi:** Am in Cd pool

#41 **xCmcli:** Cm in salt, **xCmedpi:** Cm in Cd pool

#42 **xRE1cli:** RE1 in salt, **xRE1cdpi:** RE1 in Cd pool

#43 **xRE2cli:** RE2 in salt, **xRE2cdpi:** RE2 in Cd pool

#44 **xZrccli:** Zr in salt, **xZrcdpi:** Zr in Cd pool

#45 **xNMcli:** NM in salt

#46 **xCdcli:** Cd in salt

#47 **xFecli:** Fe in salt

#48 **xLiCdi:** Li in Cd-Li anode

(20) Line #49: iR resistance between the electrodes in the unit of ohm.

ohma: Ref-Anode, **ohmc:** Ref-Solid and Graphite cathode

(21) Line #50: **effa:** Anode efficiency, **effcl:** Chlorination efficiency,

Pgcl: Chlorine pressure (Pa), **Pgox:** Oxygen pressure (Pa), **Sg:** Melt-gas reaction area (cm²)

Sr: Melt-Crucible reaction area (cm²), **k_c:** Rate constant of Melt-Crucible reaction (cm/min/Pa)

(22) Line #51: **effc:** Electrochemical efficiency, **effSld:** Solid cathode physical efficiency, **effCd:** Cd cathode physical efficiency

(23) Line #52; recovery: Redissolution rate of fallen deposit

(24) Line #53: **tmax:** Max time(s), **nts:** Number of step, **itime:** Number of input,

factSc: Increase factor of cathode surface area

(25) Line #54 - 56: Time history data

time: Time (s), **I:** Current (A), **vgCl:** Chlorine supply (L/s)

Anode: -1/0/1/2/3/4=Chlor/Graphite/Anodic/Cd/Basket/CdLi,

Cathode: -1/0/1/2=Chlor/Graohite/Solid/Cd

Line #55: **time, I, vgCl, Anode, Cathode**

Line #56: **time, I, vgCl, Anode, Cathode**

(26) Line #57- 70: Plotter control data

tfact: Factor of time axis, **tmin:** Min. time, **tmax:** Max.

Line #58: **ifact:** Current factor, **imin:** Min. current, **imax:** Max.

Line #59: **vamin:** Min. anode potential, **vamax:** Max.

Line #60: **vcmin:** Min. cathode potential, **vcmax:** Max.

Line #61: **vmin:** Min. cell voltage, **vmax:** Max.

Line #62: **smin:** Min. salt conc., **smax:** Max.

Line #63: **cmin:** Min conc. in Cd pool, **cmax:** Max

Line #64: **dfactUPu:** Factor for U&Pu, **dfactMA:** MA, **dfactFP:** FP

Line #65: **dmin:** Min. deposition weight, **dmax:** Max.

Line #66: **sfact:** Factor of spent fuel weight, **sfmin:** Min. weight, **sfmax:** Max.

Line #67: **MOXmin:** Min. MOX deposit, **MOXmax:** Max.

Line #68: **Pumin:** Min. Pu enrichment, **Pumax:** Max.

Line #69: **nps:** Output and save data interval

(40) Line #71-xx: Experimental data for comparison in plot

Line #71- xx: No. of Cell Voltage Exp data

Label#color no.# if any

No. of time history data if any

time, cell voltage if any

Line #xx - xx: No. of Conc in salt Exp data

Label#color no.# if any

No. of time history data if any

time, conc. in salt if any

Line #xx - xx: No. of Conc in Cd pool Exp data

Label#color no.# if any

No. of time history data if any

time, conc in Cd pool if any

Line #xx - xx: No. of deposit weight Exp data

Label#color no.# if any

No. of time history data, Multiple factor if any

time, deposit weight if any

Table 3-1 Input data for JURA (1/3)

No.	Example	Explanation
1	MOX codeposition	Title of the calculation
2	923	Temperature (K)
	+2 -1.069 0.499 1.62E-3 1840	<u>z: number of mole equivalents of the ion</u> <u>a,b : Ef=a+b*T/1000 (vs Cl)</u> <u>A,B : D=A*10^{^-B/T} (cm²/s)</u>
3		z, a, b, A, B for UO ₂ ion
4	+4 -2.775 0.579 4.79E-3 2480	z, a, b, A, B for U ion
5	+2 -0.414 0.654 1.62E-3 1840	z, a, b, A, B for PuO ₂ ion
6	+4 -3.010 1.000 4.79E-3 2480	z, a, b, A, B for Pu ion
7	+2 -0.036 0.517 1.62E-3 1840	z, a, b, A, B for NpO ₂ ion
8	+4 -2.629 0.670 4.79E-3 2480	z, a, b, A, B for Np ion
9	+3 -2.795 0.0 2.24E-3 1960	z, a, b, A, B for Am ion
10	+3 -2.831 0.0 2.24E-3 1960	z, a, b, A, B for Cm ion
11	+3 -3.693 0.8017 1.0E-5 0.0	z, a, b, A, B for RE1 ion
12	+3 -3.750 0.8561 1.0E-5 0.0	z, a, b, A, B for RE2 ion
13	+3 -1.212 0.9 1.0E-5 0.0	z, a, b, A, B for NM ion
	500.0 0.0 0.0 0.0	<u>Anode area (cm²)</u> Sa: Cd pool, Sb: Anode basket, ScdLi: Cd-Li anode, Sw: Zr deposit on ER wall as anode
14		
	50.0 0.0	<u>Cathode area(cm²)</u> Sc: Solid cathode, Scd: Cd cathode
15		
	1.0	Sk: Surface factor for Cd pool dissolution
16		
	0.01 0.0 0.0 0.0	<u>Anode Diffusion Layer Thickness (cm)</u> dLBkt: Anode basket ,dLCdcl: Cd pool salt side, dLCdcd: Cd pool Cd side , dLWcl: ER wall
17		
	0.01 0.0 0.0	<u>Cathode Diffusion Layer Thickness (cm)</u> dLSld: Solid cathode, dLCdcl: Cd cathode salt side, dLCdcd: Cd cathode Cd side
18		
19	1	nRE1: Selection of lanthanide 1=Ce; 2=Nd; 3=La; 4=Gd
20	2	nRE2: Selection of lanthanide 1=Ce; 2=Nd; 3=La; 4=Gd
21	1	nNM: Selection of noble metal 1=Rh; 2=Ru; 3=Pt
	0.0 0.0	<u>Initial amount in Spent fuel (g)</u> UOsf: UO ₂ , Usfi: U
22		
	0.0 0.0	PuOsf: PuO ₂ , Pusfi: Pu
23		
	0.0 0.0	NpOsf: NpO ₂ , Npsfi: Np
24		
	0.0	Amsfi: Am
25		
	0.0	Cmsfi: Cm
26		
	0.0	RE1sfi: RE1
27		
	0.0	RE2sfi: RE2
28		
	0.0	NMsfi: Noble metal
29		
	0.0	Zrsfi: Zr
30		
	0.0	Fesfi: Fe
31		
	2000.0	Total Salt inventory (g)
32		
	0.0	Cdp: Total Cd in Cd pool(g)
33		
	0.0	Cdc: Amount of Cd in Cd cathode(g)
34		
	0.0	CdLiBk: Amount of Cd-Li in Cd-Li anode(g)
35		
	3	<u>iSalt: Selection of salt</u> 1=LiCl-KCl; 2=NaCl-KCl; 3=NaCl-2CsCl; 4=NaCl-KCl-CsCl
36		

Table 3-1 Input data for JURA (2/3)

	Example	Explanation
37	12.6 0.0 0.0	<u>Initial concentration (wt%)</u> xUOcli: UO ₂ in salt, xUcli: U in salt, xUcdpi: U in Cd pool
38	0.0 3.1 0.0	xPuOcli: PuO ₂ in salt, xPucli: Pu in salt, xPucdpi: Pu in Cd pool
39	0.1 0.0 0.0	xNpOcli: NpO ₂ ion, xNplici: Np ion, xNpcdpi: Np in Cd pool
40	0.25 0.0	xAmcli: Am in salt, xAmcdpi: Am in Cd pool
41	0.0005 0.0	xCmcli: Cm insalt, xCmcdpi: Cm inCd pool
42	0.08 0.0	xRE1cli: RE1 in salt, xRE1cdpi: RE1 in Cd pool
43	0.001 0.0	xRE2cli: RE2 in salt, xRE2cdpi: RE2 in Cd pool
44	0.0 0.0	xZrccli: Zr in salt, xZrcdpi: Zr in Cd pool
45	0.003	xNMcli: NM in salt
46	0.0	xCdcli: Cd in salt
47	0.0	xFecli: Fe in salt
48	0.0	xLiCdi: Li in Cd-Li anode
49	0.0 0.0	<u>iR resistance (ohm) between the Electrodes</u> ohma: Ref-anode, ohmc: Ref-cathode
50	0.7 0.1 34500 31000 641 500 4.3E-7	effa: Anode efficiency, effcl: Chlorination efficiency, Pgcl: Chlorine pressure (Pa), Pgox: Oxygen pressure (Pa), Sg:Melt-gas reaction area (cm ²), Sr:Melt-crucible reaction area(cm ²),
51	1.0 1.0 0.5	effc: electrochemica efficiency, effSld: Solid cathode physical, efficiency, effCd: Cd cathode physical efficiency
52	1.0	recov: Fraction of fallen deposite dissolove in Salt
53	36000 100 3 1.0	tmax: Max time(s), nts: Number of step, itime: Number of input, factSc: Increase factor of cathode surface area
54	0.0 5.0 0.0 0 0	time: Time (s) , I: Current(A), vgCl: Chlorine supply (L/s) Anode: -1/0/1/2/3/4=Chlor/Graphite/Anodic/Cd/Basket/CdLi, Cathode: -1/0/1/2=Chlor/Graohite/Solid/Cd
55	18000. 5.0 0.0 0 0	time, I, vgCl, Anode, Cathode
56	36000. 5.0 0.0 0 0	time, I, vgCl, Anode, Cathode
57	3600. 0.0 10.0	<u>Plotter control data</u> tfact: Factor of time axis, tmin: Min. time, tmax: Max.
58	1.0 0.0 20.0	ifact: Current factor, imin: Min. current, imax: Max.
59	-2.0 2.0	vamin: Min. anode potential, vamax: Max.
60	-2.0 2.0	vcmin: Min. cathode potential, vcmax: Max.
61	0.0 2.0	vmin: Min. cell voltage, vmax: Max.
62	0.0 20.0	smin: Min. salt conc., smax: Max.
63	0 2.0	cmin: Min conc. in Cd pool, cmax: Max
64	1.0 10. 100.	dfactUPu: Factor for U&Pu, dfactMA: MA, dfactFP: FP
65	0.0 500.0	dmin: Min. deposition weight, dmax: Max.
66	1000.0 0.0 50.0	sffact: Factor of spent fuel, sffmin: Min. weight, sffmax: Max.
67	0.0 500.0	MOXmin: Min. MOX deposit, MOXmax: Max.
68	0.0 50.0	Pumin: Min. Pu enrichment, Pumax: Max.
69	10	nps: Output and save data interval

Table 3-1 Input data for JURA (3/3)

	Example	Explanation
	0	<u>Experimental data input</u>
70		No. of Cell Voltage Exp data
xx	3	No. of Conc in salt Exp data
xx	Exp UO2#3#	Label#Color No.#
xx	3	No. of Time History data
xx	0 12.6	time, conc.
xx	18000. 7.8	time, conc.
xx	36000. 3.8	time, conc.
xx	Exp PuO2+Pu#5#	Label#Color No.#
xx	3	No. of Time history data
xx	0 3.1	time, conc.
xx	18000. 2.6	time, conc.
xx	36000. 2.0	time, conc.
xx	Exp NpO2#7#	Label#Color No.#
xx	3	No. of Time History data
xx	0 0.1	time, conc.
xx	18000. 0.03	time, conc.
xx	360000. 0.015	time, conc.
xx	0	<u>No. of Conc in Cd pool Exp data</u>
xx	3	<u>No. of Deposit weight Exp data</u>
xx	Exp UO2#3#	Label#Color No.#
xx	1 1.0	No. of Time History, Multiple factor
xx	36000. 208.	time, deposit
xx	ExpPuO2#5#	Label#Color No.#
xx	1 1.0	No. of Time History, Multiple factor
xx	36000. 51.1	time, deposit
xx	Exp NpO2X10#7#	Label#Color No.#
xx	1 10.0	No. of Time History, Multiple factor
xx	36000. 1.84	time, deposit

4. Sample calculations

(1) MOX co-deposition by the oxide pyro-process

Sample calculation results of the MOX co-deposition in the oxide pyro-process are shown in Fig. 4-1 to Fig.4-6. The experiment was performed in RIAR⁵⁾. The cell voltage is slightly increased due to the decrease of the cathode potential as shown in Fig. 4-1. All the anode current is consumed to produce the chlorine gas as shown in Fig.4-2, while both the UO_2 and PuO_2 ions are reduced at the cathode as shown in Fig. 4-3. The concentration of UO_2 ion keeps decreasing and that of PuO_2 ion is very small as shown in Fig. 4-4. UO_2 , PuO_2 and NpO_2 are deposited on the cathode as shown in Fig. 4-5. The Pu enrichment at each time is plotted by line #2 and that of integrated average from the beginning is also plotted by line #1 in Fig. 4-6. The average Pu enrichment of the final deposit is about 12%.

(2) Solid cathode deposition by the metal pyro-process

Sample calculation results of the solid cathode deposition in the metal pyro-process are shown in Fig. 4-7 to Fig.4-12. The experiment was performed in ANL⁶⁾. The Cell voltage is compared with the experimental data in Fig. 4-7. The contributions of each ion to the anode current and the cathode current are plotted in Figs. 4-8 and 4-9 respectively. Concentration of ions in the melt is compared with the experimental data in Fig. 4-10. Concentration of elements in the Cd pool is also compared with the experimental data in Fig. 4-11. Time history of the cathode deposition is compared with the experimental data in Fig. 4-12.

(3) Cd cathode deposition by the metal pyro-process

Sample calculation results of the Cd cathode deposition in the metal pyro-process are shown in Fig. 4-13 to Fig.4-15. The experiment was performed in ANL⁶⁾. The concentration of ions in the melt and in the Cd pool is plotted in Figs. 4-13 and 4-14 respectively. Time history of the deposition into the Cd cathode is plotted in Fig. 4-15.

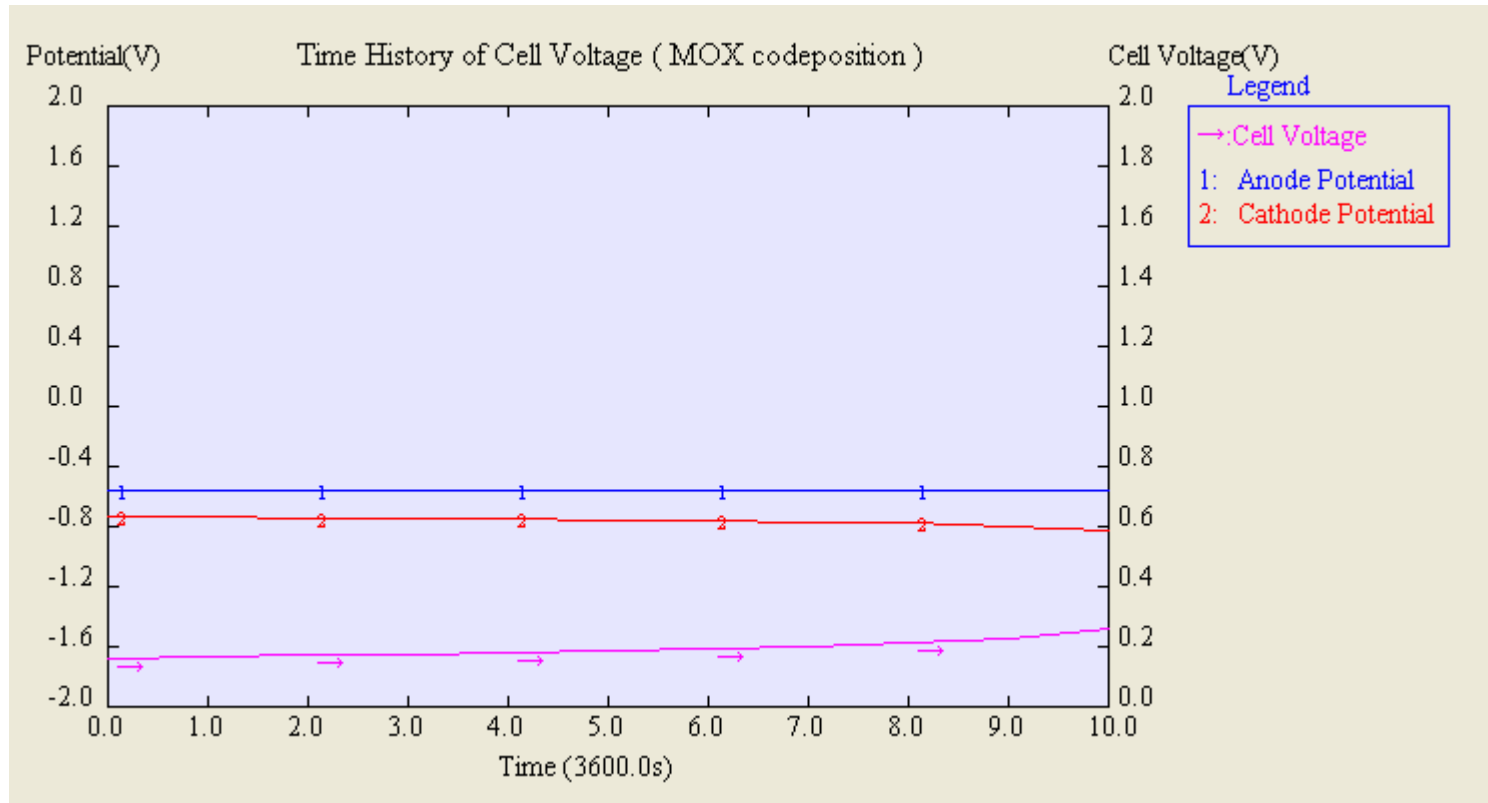


Fig. 4-1 Time history of Cell voltage in MOX co-deposition

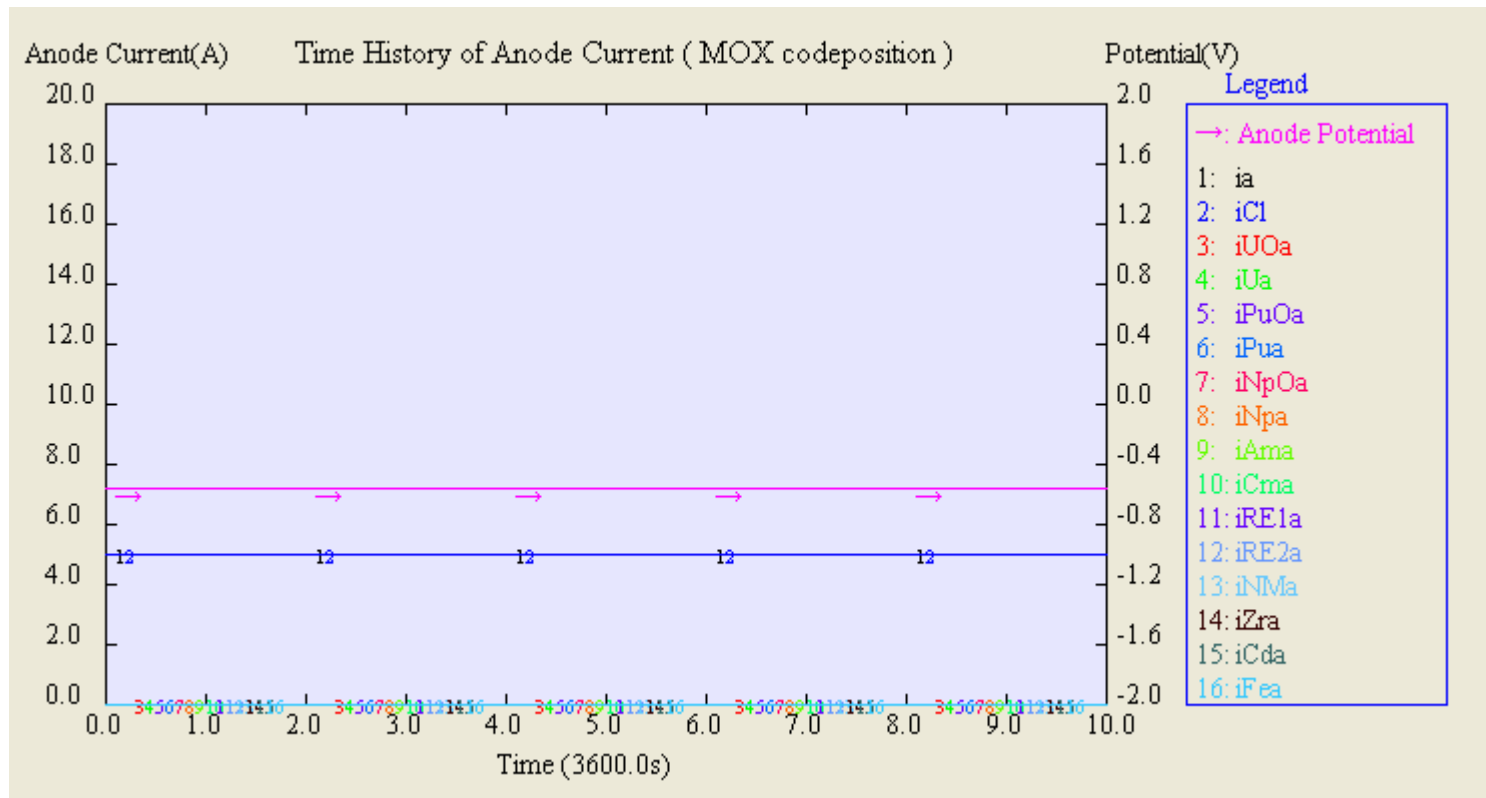


Fig. 4-2 Time history of Anode current in MOX co-deposition

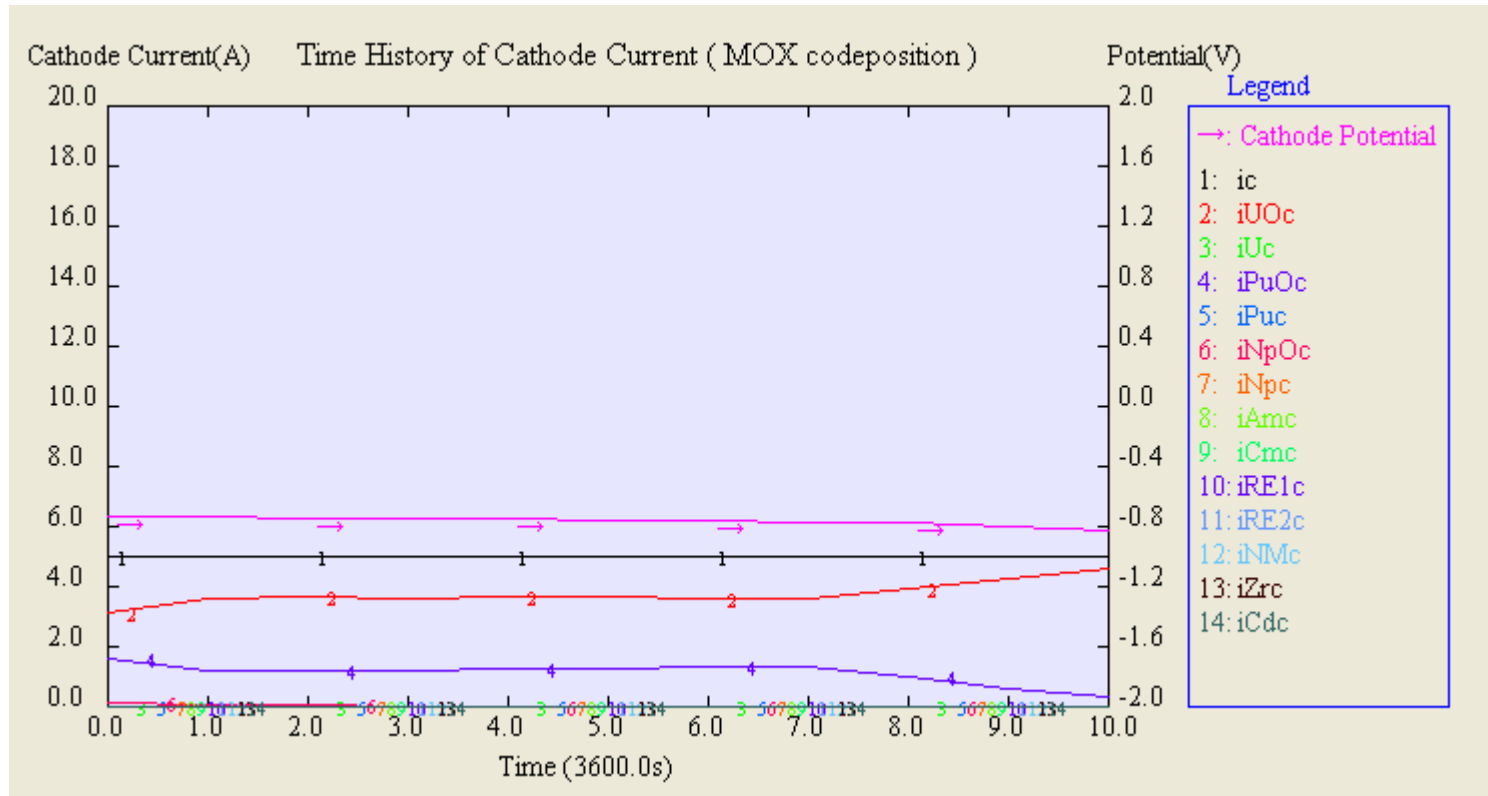


Fig. 4-3 Time history of Cathode current in MOX co-deposition

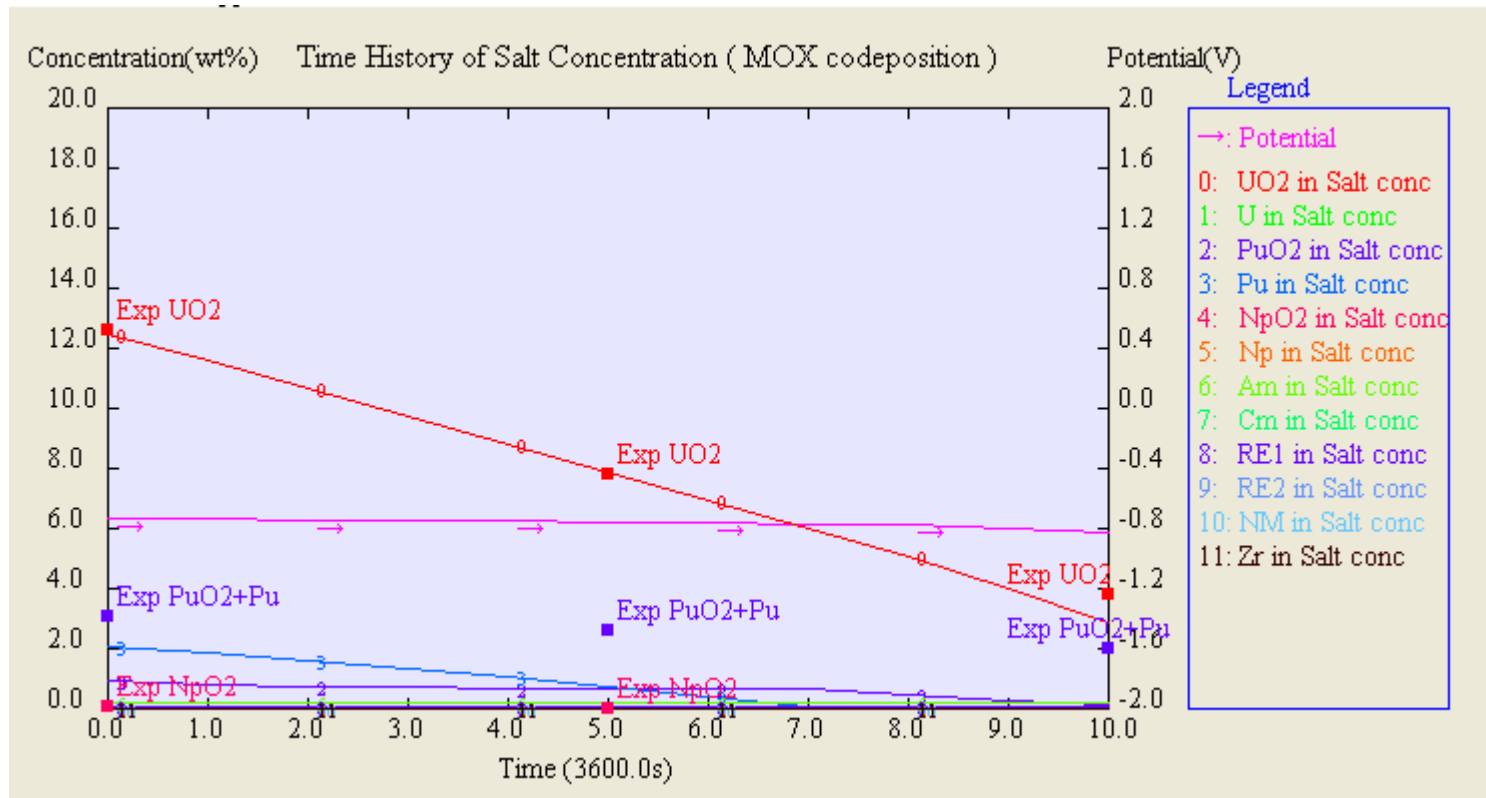


Fig. 4-4 Time history of salt concentration in MOX co-deposition

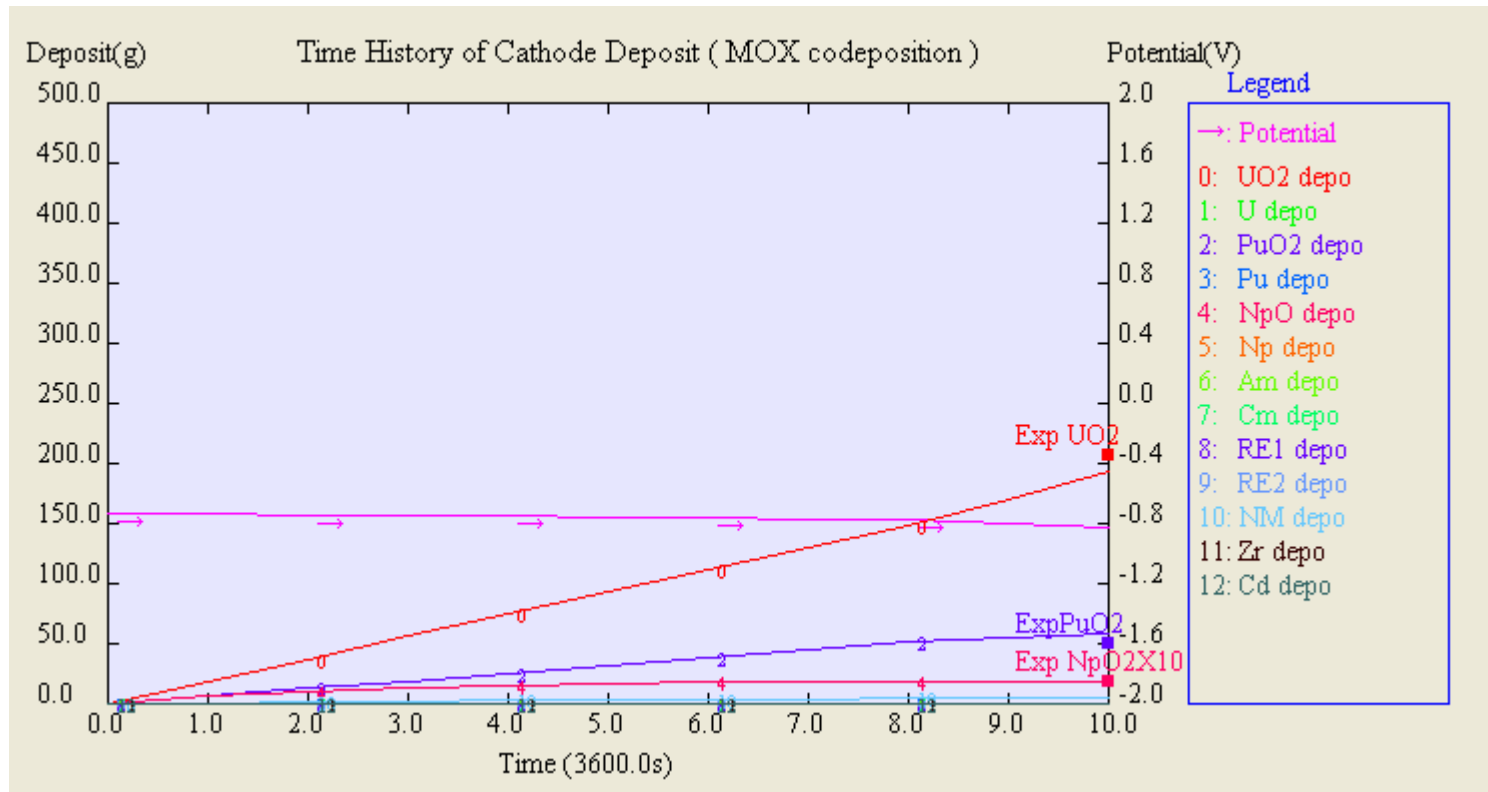


Fig. 4-5 Time history of cathode deposit in MOX co-deposition

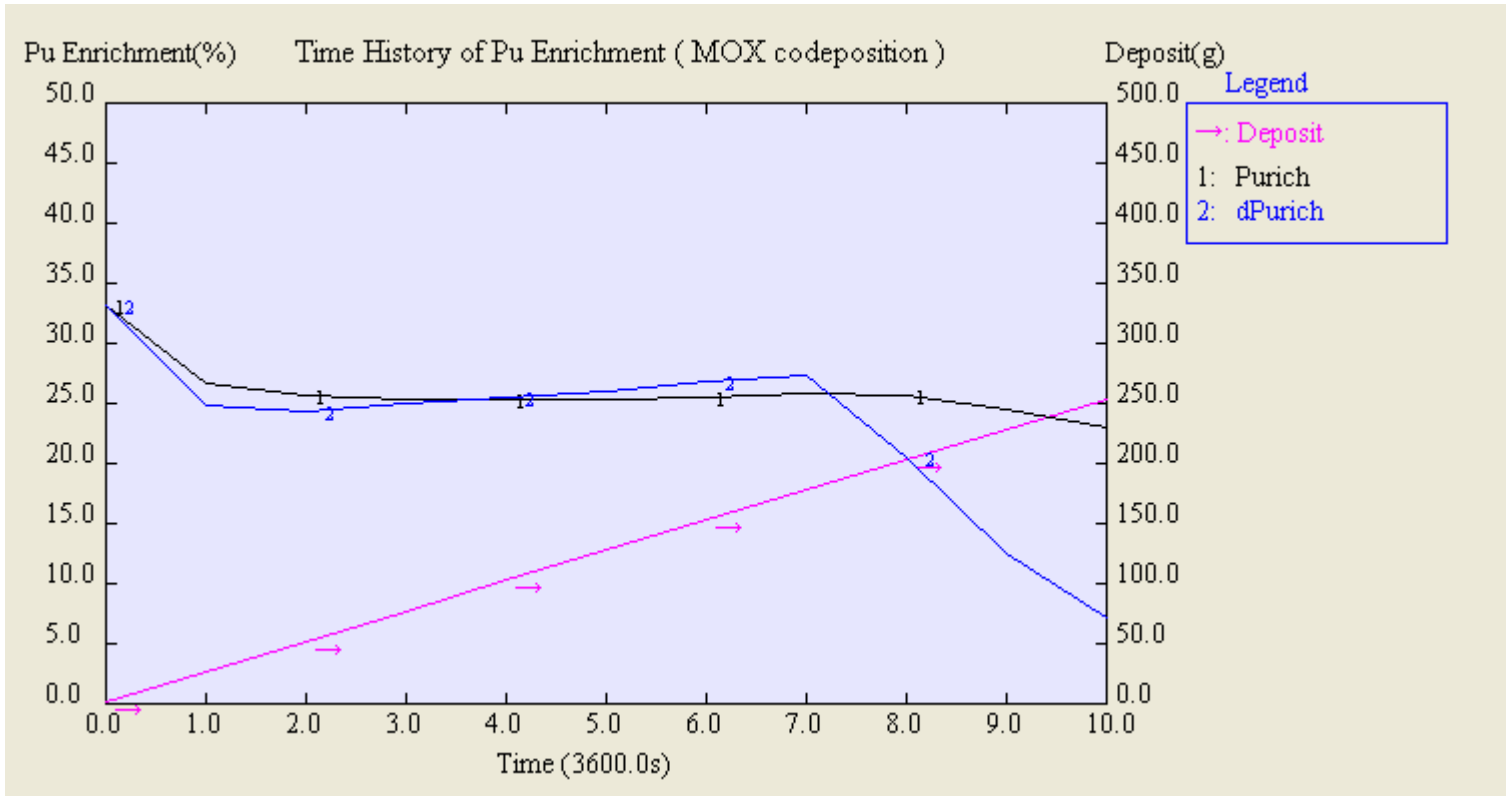


Fig. 4-6 Time history of Pu enrichment in MOX co-deposition

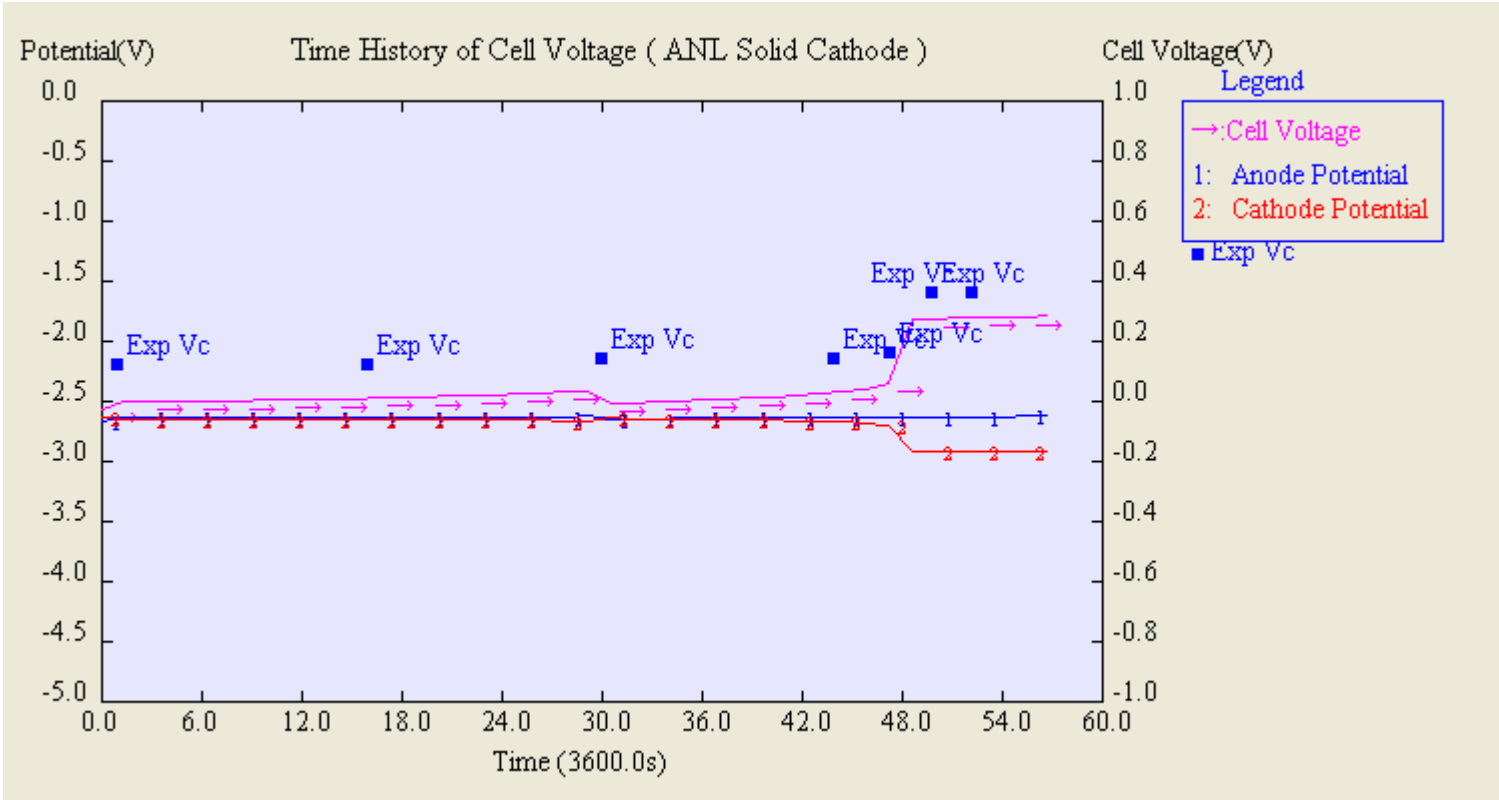


Fig. 4-7 Time history of Cell voltage in Solid cathode deposition

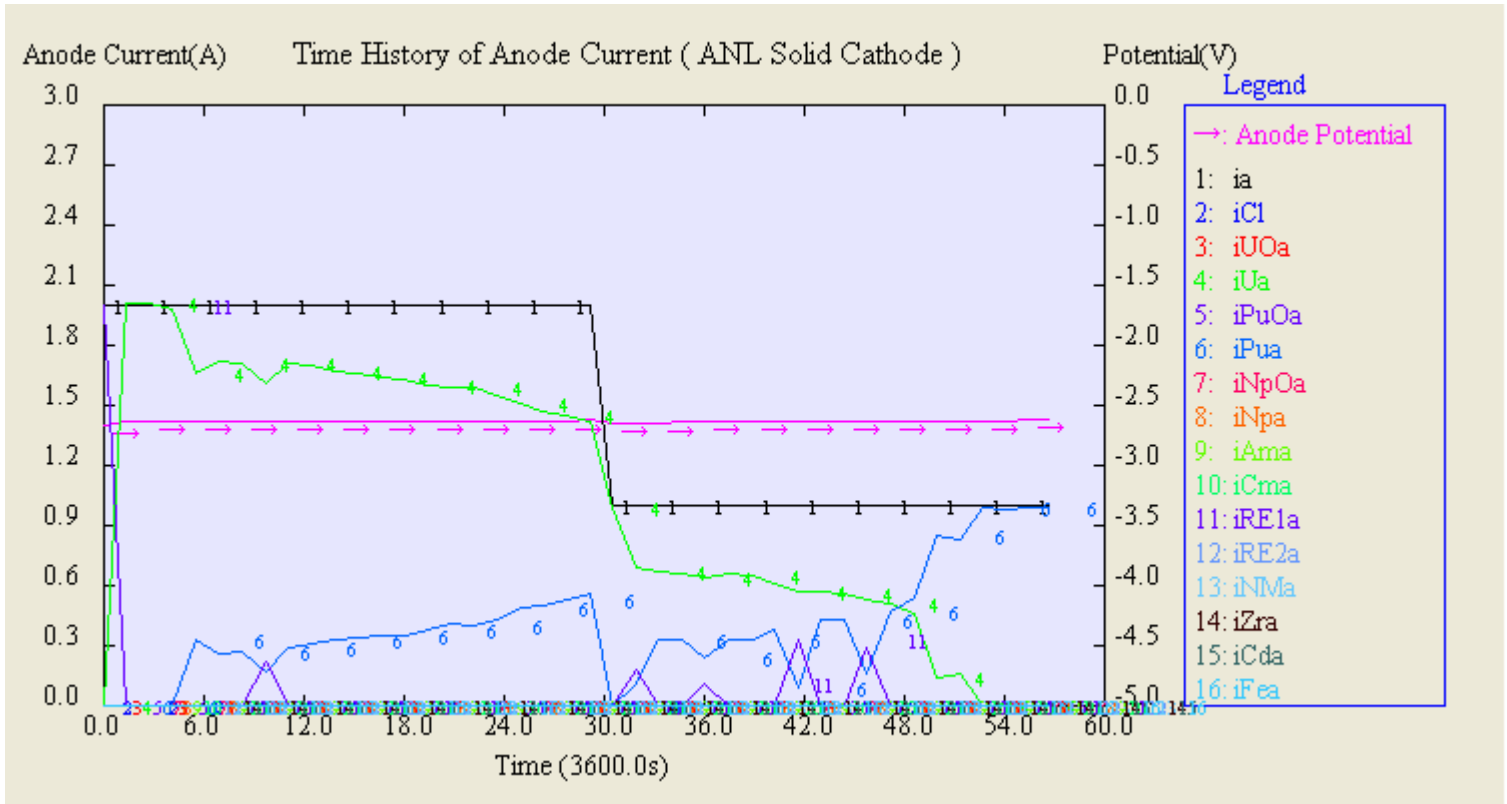


Fig. 4-8 Time history of Anode current in Solid cathode deposition

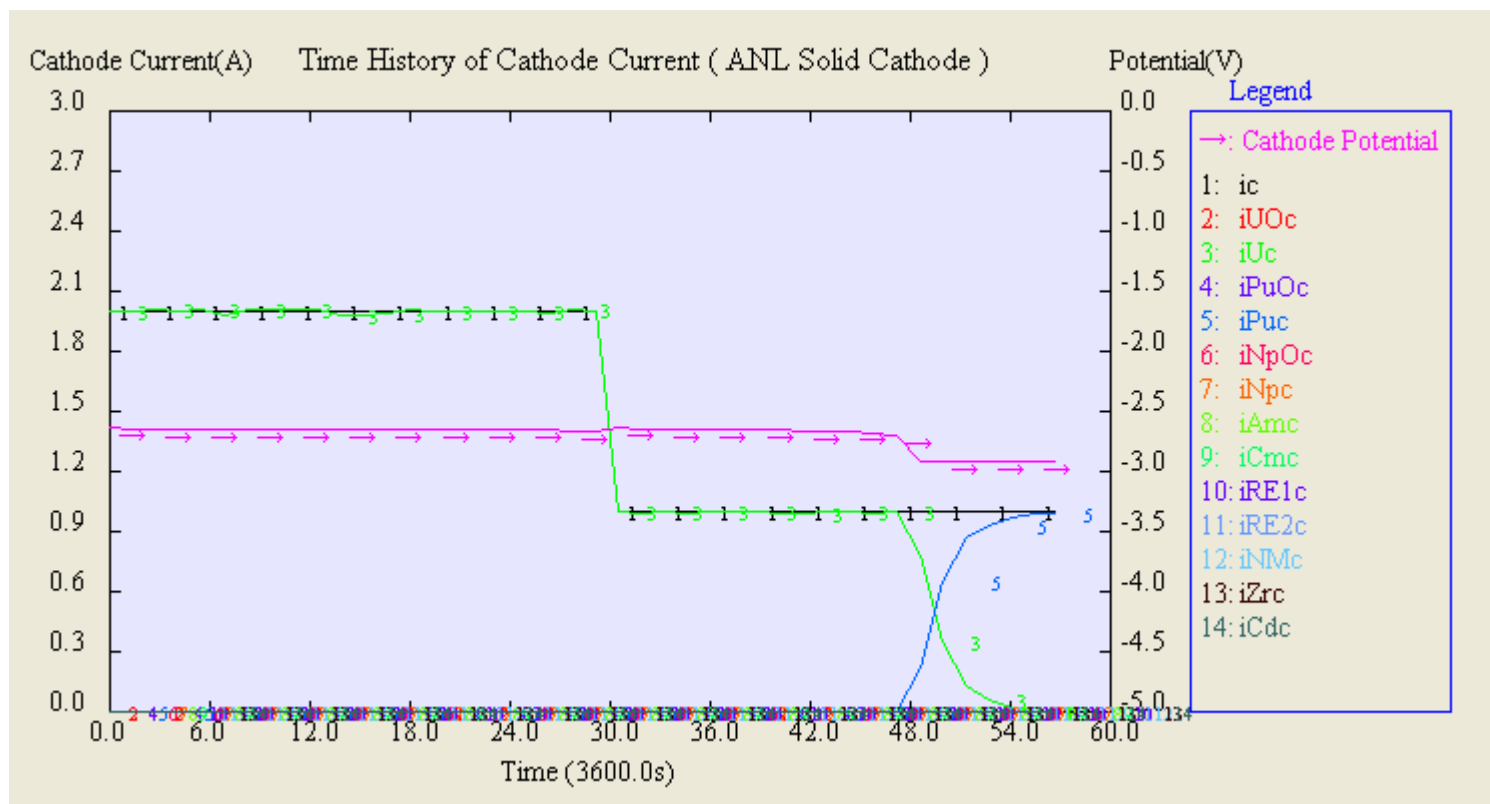


Fig. 4-9 Time history of Cathode current in Solid cathode deposition

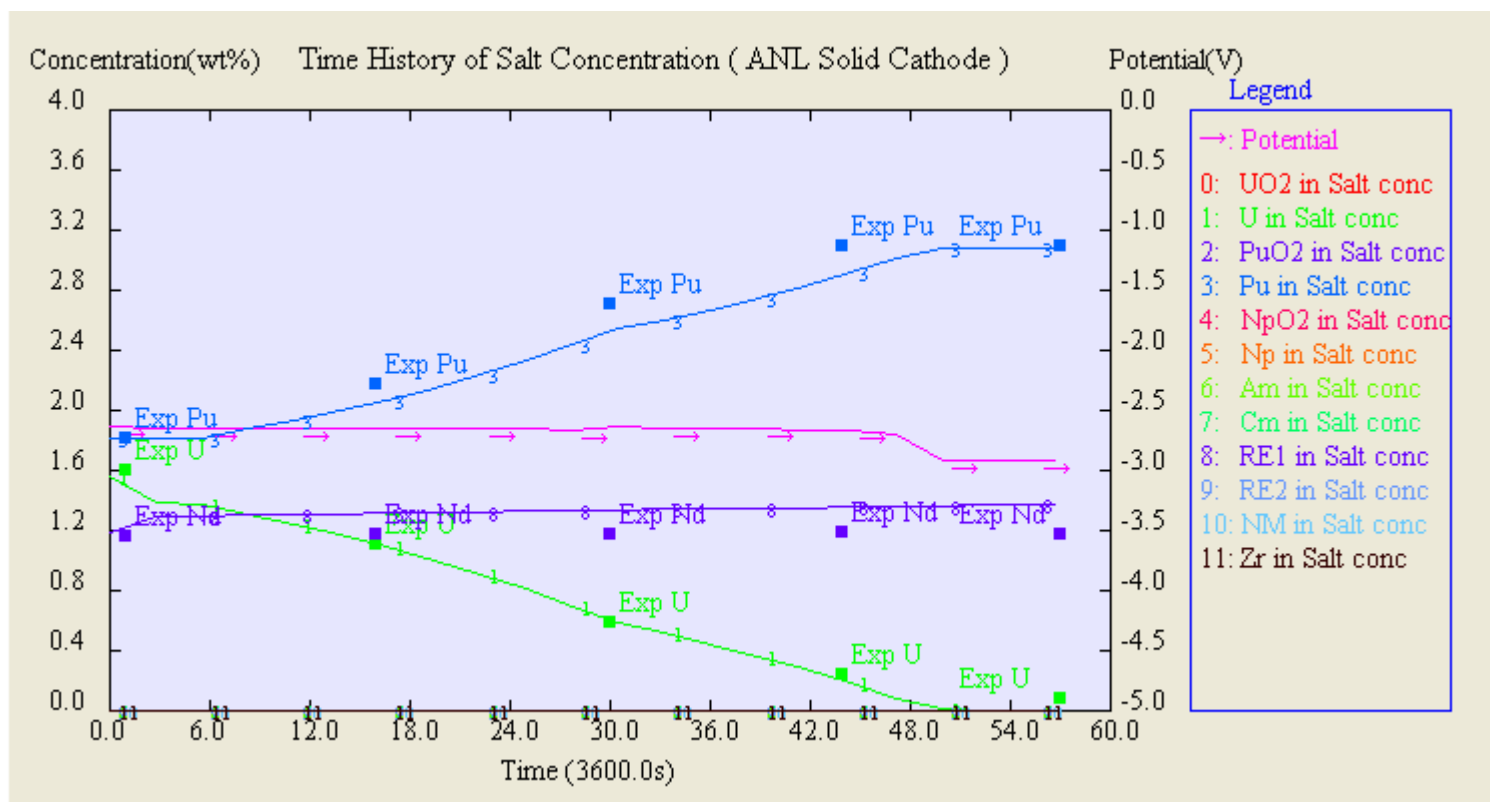


Fig. 4-10 Time history of salt concentration in solid cathode deposition

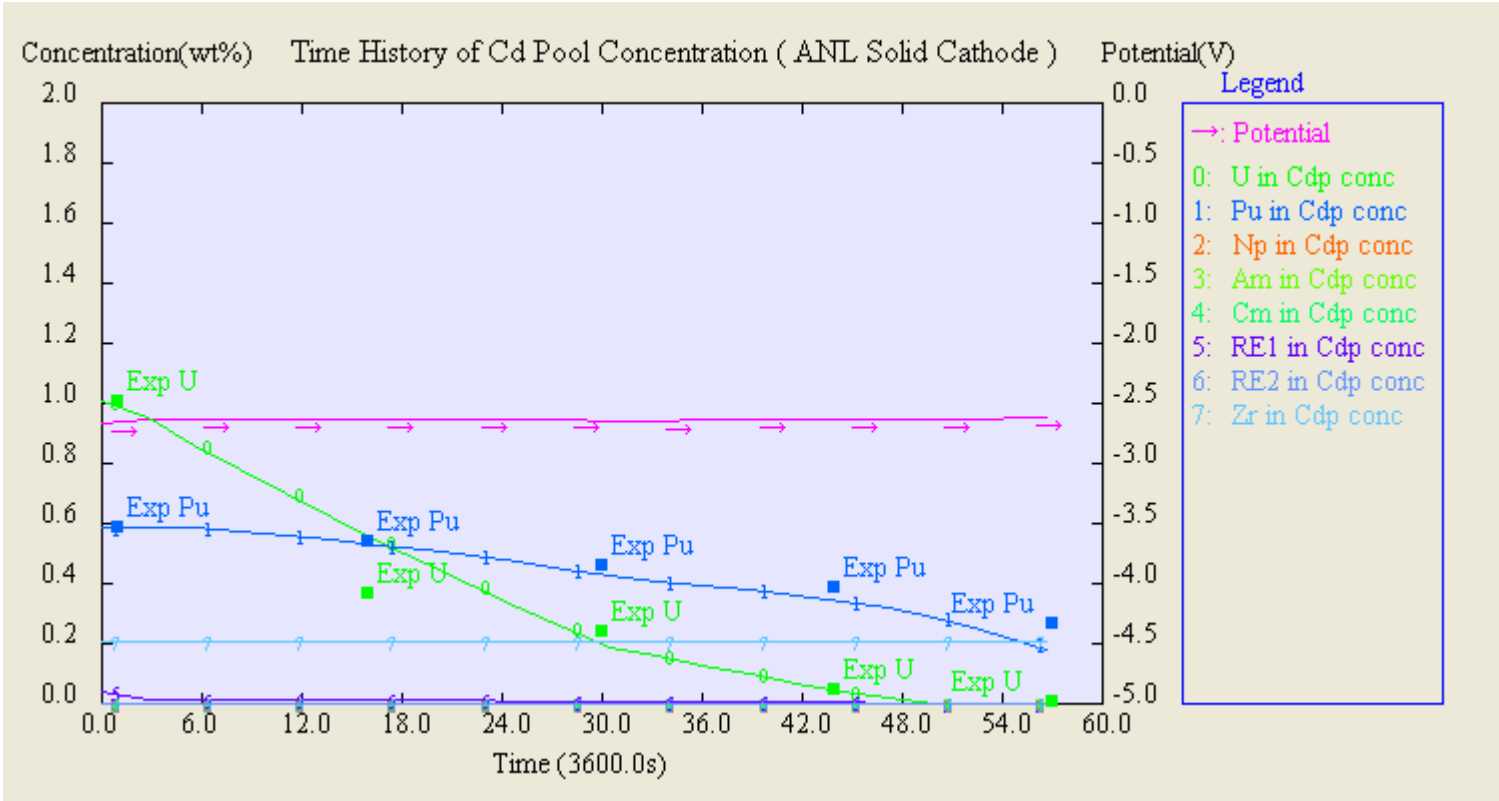


Fig. 4-11 Time history of Cd pool concentration in solid cathode deposition

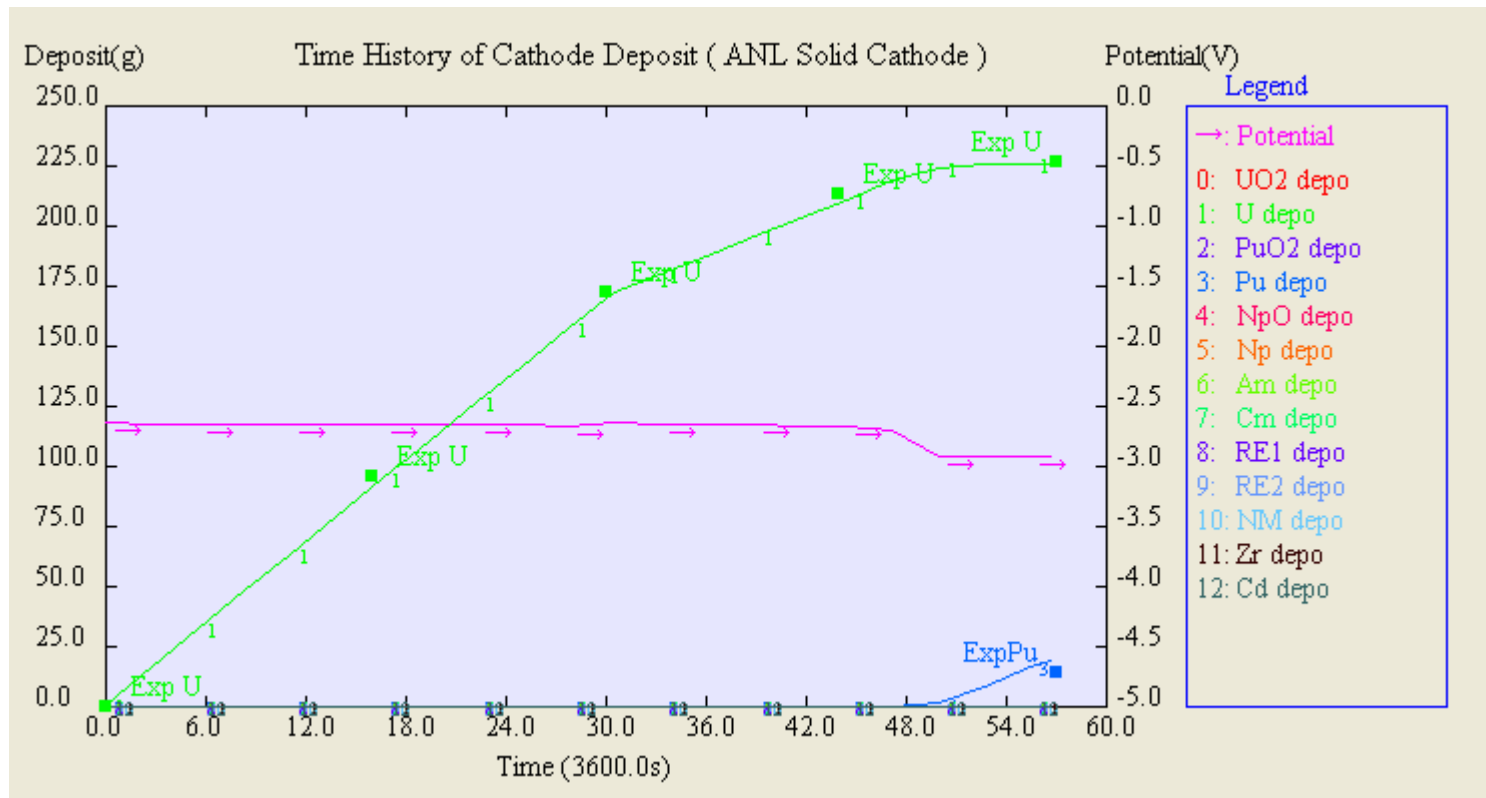


Fig. 4-12 Time history of cathode deposit in solid cathode deposition

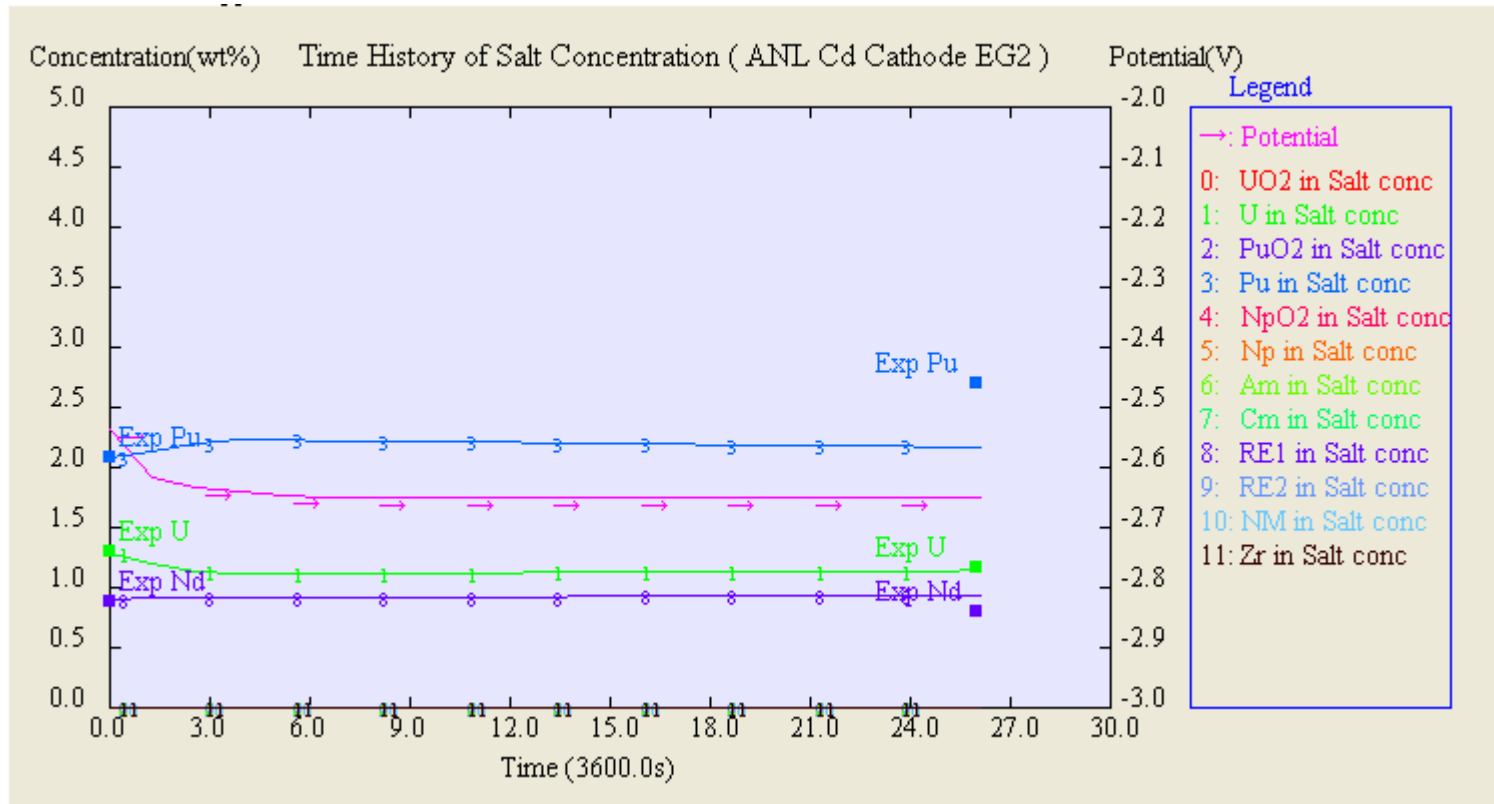


Fig. 4-13 Time history of salt concentration in Cd cathode deposition

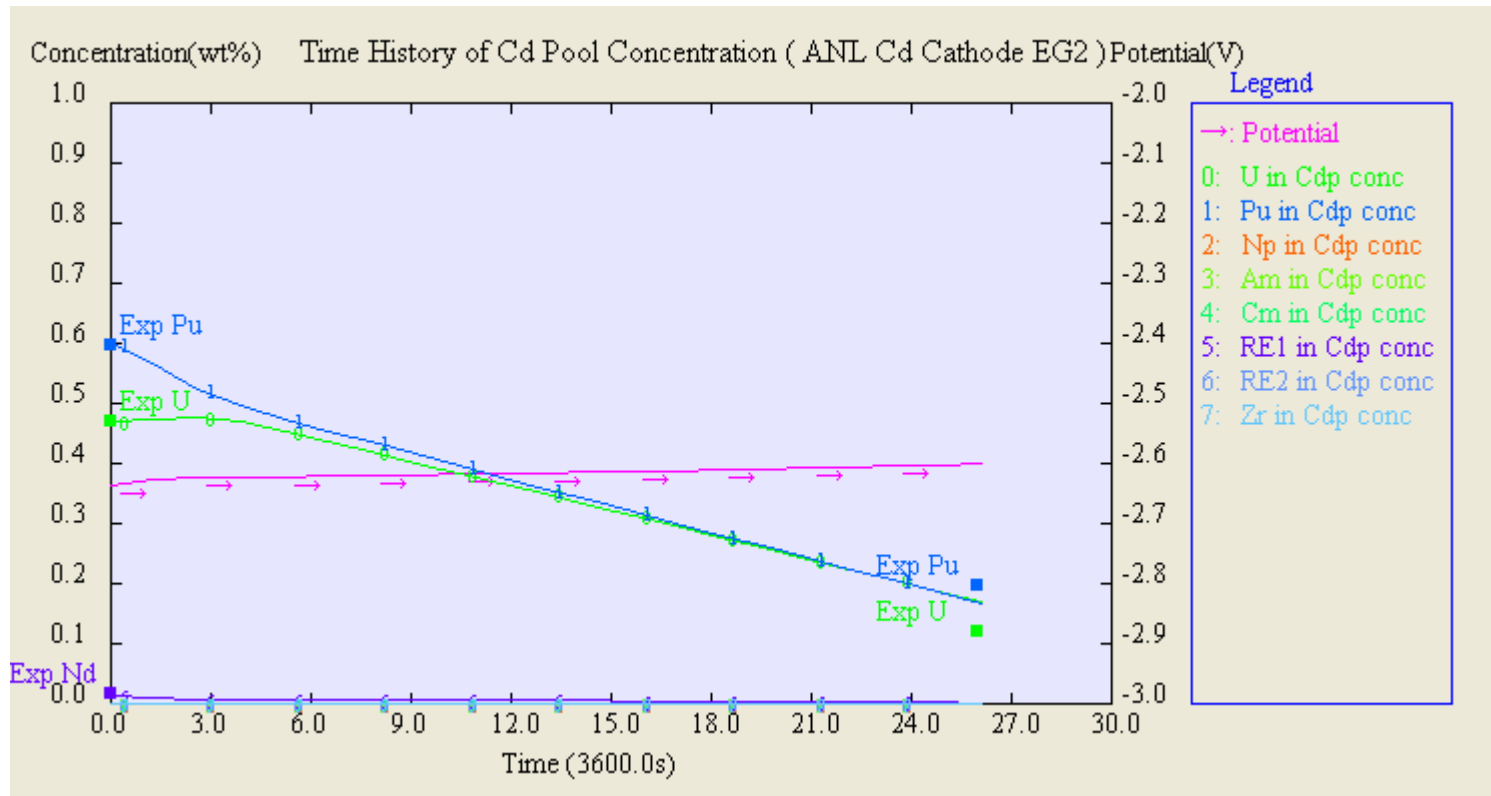


Fig. 4-14 Time history of Cd pool concentration in Cd cathode deposition

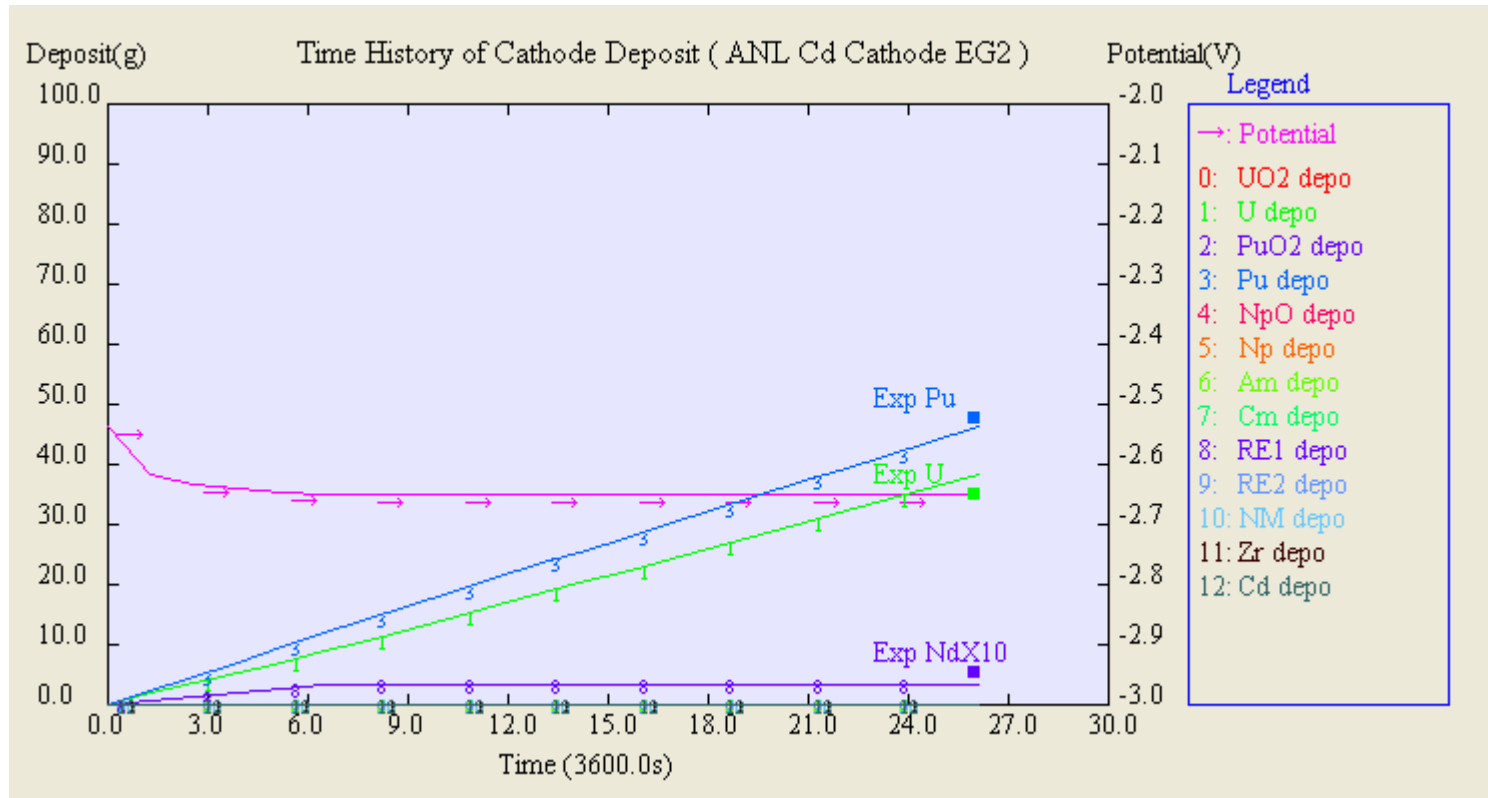


Fig. 4-15 Time history of cathode deposit in Cd cathode deposition

5. References

- 1) A. Kawabe, T.Kobayashi “ Development of PALEO code” to be presented in GLOBAL '97 (1997).
- 2) T. Kobayashi et al. “Evaluation of Cd pool potential in a electrorefiner with ceramic partition for spent metallic fuel”, J. nucl. science and tec., vol/34, no.1, pp50-57, (1997).
- 3) T. Kobayashi “Analytical evaluation of molten salt electro-refining of spent nuclear fuels”, Ph. D thesis for Tohoku University (1999).
- 4) S. K. Vavilov et al. “Thermodynamics of redox and electrode reactions of Plutonium in a melt of NaCl-CsCl eutectic mixture”, Radiokhimiya vol. 27. No.1, pp.116-121, Jan.-Feb., (1985).
- 5) M. V. Kormilizyn et al. “Pyro-electrochemical reprocessing of irradiated MOX Fast Reactor Fuel IV Testing of the reprocessing process with direct MOX fuel production” to be presented in GLOBAL '99, (1999).
- 6) T. Kobayashi “ Development of TRAIL, a simulation code for the molten salt electrorefining of spent nuclear fuel”, J. alloys and compounds, 197, pp7-16, (1993).
- 7) S. K. Vavilov private communication(2003)